Game-Theoretic Approach with Cost Manipulation to Vehicular Collision Avoidance

Christopher C. Howells

Thesis submitted to the Faculty of the
Virginia Polytechnic Institute and State University
in partial fulfillment of the requirements for the degree of

Master of Science
in
Electrical Engineering

Dr. Pushkin Kachroo, Chair
Dr. A. L. Abbott
Dr. W.T. Baumann

May 13, 2004
Blacksburg, VA

Keywords: collision avoidance, differential games, autonomous vehicle, intelligent transportation system

Game-Theoretic Approach with Cost Manipulation to Vehicular Collision Avoidance

Christopher C. Howells

(ABSTRACT)

Collision avoidance is treated as a game of two players with opposing desiderata. In the application to automated car-like vehicles, we will use a differential game in order to model and assess a worst-case analysis. The end result will be an almost analytic representation of a boundary between a "safe" set and a "unsafe" set. We will generalize the research in [27] to non-identical players and begin the setup of the boundary construction. Then we will consider the advantages and disadvantages of manipulation of the cost function through the solution and control techniques. In particular, we introduce a possible way to incorporate a secondary objective such as sticking to a straight path. We also look a hybrid technique to reduce steering when the opposing player is out of the reach of the vehicle; i.e., is out of the "unsafe" set and less extreme maneuvers may be desired.

We first look at a terminal cost formulation and through retrograde techniques may shape this boundary between the "safe" and "unsafe" set. We would like this research, or part thereof, to be assessed and simulated on a simulation vehicle such as that used in the Flexible Low-cost Automated Scaled Highway (FLASH) at the Virginia Tech Transportation Institute (VTTI). In preparation, we briefly look at the sensor demands from this game-theoretic approach.

Acknowledgements

The author would like to thank all those who had some input into this research; the research group for their support, and in particular Patricia and Mark for their wisdom; anyone who reads this and gives me feedback; Ian Mitchell, Claire Tomlin, and Shankar Sastry for their help; Paco for his word; my family's support; and of course Pushkin Kachroo for all his help and guidance whose wisdom is only surpassed by Yoda.

List of Figures and Tables

Table of Contents

Chapter 1

Introduction

In many cases a car, even when driven properly, end in collision. There are situations where other vehicles are under the control of inebriated drivers, objects such as cats, dogs, deer, squirrels, etc., and even stationary objects, and dangerous upcoming curves in the road that endanger the vehicle and any of its passengers. Vehicular collision consequences can be severe. According to the 1998 Fatality Analysis Reporting System (FARS), there were 6.3 million police reported crashes, of which over 40,000 resulted in fatalities, in the U.S. Moreover, fatalities grew to over 42,000 by 2002 [1][2]. From 1992-1996 to 1997-2001, the number of passenger car vehicle wrecks rose 4 percent, while the number of sport utility vehicle wrecks rose 69 percent.

Collision avoidance is one of the ultimate goals of automobile safety. Improving safety, a self-interest objective, obviously dates back in time. Safety belts have been around since 1849; though, it wasn't until 1930 that automobile manufacturers began to install seat belts as standard equipment [3]. Safety made its way with the invention of air bags, anti-lock brakes, better materials, and safer structural designs. With the increase of faster cars, more traffic, and more distractions, safety must move to the next level in an effort to reduce the awesome statistics mentioned above.

This is projected in the research being done for automated highways in which vehicles are controlled solely through computers. And this research lends new safety innovations to contemporary vehicles paving the way to more automatic control. Collision avoidance is the number one example since systems may be designed for completely automated vehicles while other systems could be designed for today's vehicles without severely relinquishing the driver's controls. However, we focus our attention to automated vehicles in hopes of its use for automated highways but also its extrapolation to more "passive" systems.

1.1 Past and Current Research in FLASH

Automated highway systems are a big and expanding research area. Many different controllers and sensor systems have been designed in order to control the motion of an actual vehicle. The FLASH team is a part of this effort in designing and utilizing a small-scale test bed to assess different aspects of an automated highway. Research is devoted to devise effective and efficient ways of controlling the overall system. For example, a kinematic model in [4] is designed to decouple steering and velocity inputs. A dynamic model in [5] also accounts for the dynamics of the steering and velocity actuators. There

is also current work in traction control, system integration, and hopefully image-based control. This paper adds to this work a formulation framework which could be utilized in a collision avoidance system for the FLASH vehicles.

1.1.1 Nonholonomic Constraints

Due to the maneuverability constraints of a car-like vehicle, most controllers rely upon nonlinear techniques. Some research, however, has been devoted to transforming the state equations into a form such that linear techniques may be used. Controllers may use sliding-mode, chained form, neural networks, abstraction, and hybrid strategies. Better modeling of actual vehicle dynamics is possible when slip and dynamics are considered. However, due to the increased complexity, nonholonomic constraints are ignored in the collision avoidance setup, and for avoidance purposes would not be a bad assumption.

1.1.2 Sensor Technology

An adaptive cruise control in [6] is designed and implemented showing many safety advantages. There is a great deal of research just devoted to the sensor technology involved in an automated vehicle. In order for vehicles to make correct and safe maneuvers among other vehicles, certain parameters need to be correctly measured within a certain error. Curvature is just one of these parameters and its estimation is explored in [9]. Point stabilization features and ability to track paths rely on these sensed and estimated parameters. Similarly, any collision avoidance system will also need the proper sensor technology for its demands. We will explore the demands of our system and how we may measure these parameters using the technology readily available to the FLASH team.

1.2 Outline

This paper will look at an approach to control an automated vehicle in a dangerous environment. Evasive maneuvers are likely and while we devote lesser time to tracking of vehicle, we spend more time in securing safety of vehicle through a worst-case analysis. Chapter 2 will discuss different approaches which may meet these ends, and we ultimately favor a game-theoretic approach. Chapter 3 introduces models and optimality conditions for the vehicle and a posing threat. This advances the research done in [27] and the setup in [32]. Chapter 4 then indicates the use of this approach as it applies to guaranteeing avoidance or the potential to collision through splitting the state space into a safe and unsafe set. Chapter 5 analyzes and briefly sets up the approach necessary to shape the boundary of these two sets, which would be done before any avoidance system is implemented. Chapter 6 introduces some variations to the problem and how they

might reshape the worst-case analysis in conjunction with secondary objectives. Chapter 7 discusses solving and devises control plans with the original setup and its variations. Finally, whereas the game-theory setup is not backed with any simulation results, and certain modifications and additions will be necessary for these, the ideas have been flexed from previous research in this specific genre of collision avoidance to incorporate more scenarios and less assumptions. Future work remains open as this technique is still blossoming. And it is of no surprise it will be handled since all collision avoidance systems ultimately desire a worst-case analysis and some means to model it. These thoughts are expanded in Chapter 8.

1.3 Contributions from This Thesis

- Generalize the game-theoretic approach to collision avoidance to the case of non-identical vehicles, allowing opposing object to be kinematically different than vehicle
- Integrated a path following objective with collision avoidance in a one-cost setup
- Propose a hybrid solution approach to reduced steering
- Weighed advantages and disadvantages of cost adjustment, dimension adjustment, analytic and numerical techniques for solutions

Chapter 2

Collision Avoidance Systems

This chapter discusses the many diverse designs and algorithms associated with collision avoidance. It looks mainly at those designed for robotic cars, while touching on those designed for other systems such as aircraft and water vehicles.

2.1 Passive Systems and Contemporary Automobiles

There are already many introductive systems for current vehicles. Presently, these systems are rather passive; that is, systems which provide auditory or haptic warnings, but the driver still maintains full control over the vehicle. More systems may remain passive until collision is calculated to be unavoidable, at which point they actuate the brakes to dampen the impact. These systems tend not to interfere with the driver's controls because at this point it is expected the driver will hit the brakes. It would not be easy to implement a system which shared control with its driver when the car was moving, for the system's input may conflict with the driver's input. Such systems have been implemented on a Jaguar, containing collision warning and even adaptive cruise control, which regulates a proper headway when it approaches another vehicle [7]. One system known as the virtual bumper combines longitudinal and lateral techniques to incur "virtual forces" which tend to "push" the host vehicle into a safer trajectory, though the design is intended to relinquish the majority of the control to the driver [8]. In a sense, adaptive cruise control provides collision avoidance of vehicles traveling in the same direction.

2.2 Potential Field Designs

More active designs are catered to semi- or fully automated systems. For example, in [10], one approach breaks the operation of a vehicle into two sets: normal operation when no objects are sensed and avoidance operation when objects are sensed. Unfortunately this approach suffers from chattering issues. As a result, sliding techniques in the Filipinov sense are utilized. This system and others approach the problem by defining an attractive-repulsive field, where target locations 'attract' while obstacles 'repulse'.

Other systems might plan local trajectory escapes based on any number of factors or probabilistic distributions. The *Vector Field Histogram* method for example decides

movement through direction and speed based on an angular histogram describing the density of obstacles [12].

2.3 Stochastic Designs

In [11] it is found that local planning based on range measurements instead of searching for an optimal control can be carried out much quicker, and in such a way that allows the dynamics to be taken into account. Evaluation functions employing utility functions which are defined over the neighboring state space reduce the problem to a dynamic programming one. The problem becomes one of a *Markov Decision Process* where the utility function assigns probabilistic values to each state in the state space. The solution is found optimally as the moving agent optimally receives awards from its environment [11].

Assigned probabilities can also incorporate path planning instead of local planning. These methods are useful in mid- to long-range conflict resolution systems as would be needed in a free-flight environment for airplanes. In [20], aircraft motion is modeled as a deterministic trajectory plus a scaled Brownian motion perturbation. The assigned probabilities transform into probabilities of containing the Brownian trajectory in a safe region.

Many collision avoidance systems lack the ability to predict future optimal trajectories matched against the movement of a threat, which may or may not behave optimally. Path planning has the disadvantage of being corrupted by noisy measurements, which may lead the robot astray. One way of circumventing these problems is through a risk collision avoidance system. Decision making is based on the probability density function for the relative position from the vehicle to all sensed objects. Risk is assigned by measurement uncertainty and driver maneuvers. This may also be helpful in a heavy traffic situation where measurements may be misleading [16].

2.4 Sensor Technology

Even sensor technology becomes an important aspect of collision avoidance. With different sensors comes different accuracy and different levels of recognition. Basic models may only use infrared, radar, or ultrasonic technology to acquire range and angle measurements of objects. Others may use infrared and radar to control the lateral movement of the vehicle on white lines or reflector stripe respectively. Magnetic sensors may also be used for this purpose but requires magnets to be embedded into the road. In fact, infrared and magnetic have been implemented for lateral control in the FLASH setup. For distance measurements used in the application of adaptive cruise control, FLASH utilized ultrasonic sensors, which were capable of measurements from 150mm to 2.6mm. For collision avoidance, range and angle measurements are necessary, so for any

setup that used sensors acquiring only distance measurements would requirement more than just one sensor. Price and space are both factors that must be considered. Laser radar provides more accurate and longer range measurements. Unfortunately, these measurements may pick up wanted items that may interfere with regular data logging. Imaging allows the vehicle to "see" and processing allows distinguishing different items. Imaging may also be used for lateral control by recognizing patterns placed in the road. The downside of image processing is evident in the amount of data memory required just to hold even a few frames. Monolithic Millimeter Wave Integrated Circuits (MMICs) are a solution to this problem and allow even compact systems to implement high resolution [13].

2.5 Fuzzy and Neural Network Designs

One of the most prevalent ideas is based on fuzzy neural networks. These systems must be first trained in an environment in order to perform well. However, neural networks allow much freedom in the designing and the "response" of the system is usually more versatile than with normal control methods. In [15] predefined rules are learned by the robot which acquires the capacity to avoid collisions with those of a dynamic attitude, i.e., moving objects.

Real-time collision avoidance for two autonomous vehicles can be based on non-cooperative game theory, such as in [21]. Modeled as point masses, it is assumed one vehicle plays optimally to avoid a collision while the other vehicle plays the complete opposite approach (i.e., to cause a collision) due to fatigue, drunkenness, loss of control, etc. A non-cooperative game provides a worst-case setup. Development of the model with the inputs being a curvature and acceleration selection results in the necessity for a numerical solution, which in [21] is carried out through neural networks and a German simulator called the Stuttgart Neural Network Simulator (SNNS). From three layers of perceptrons, advanced formulations are integrated and approximate optimal trajectories and singular manifolds are plotted.

In [14] neural networks are copied from the neuron structure of an ordinary cockroach which seems to sense and react superiorly to other evasive strategies. This is not surprising for anyone who has tried to kill a cockroach and noticed how difficult it was to predict its maneuvers. The cockroach escape circuit accurately identifies wind stimuli parameters gathered by mechanoreceptive hairs and conducts control through its thorax. By modeling this network, a collision avoidance system is created that could take into account multiple threats. This might be useful for vehicular collision avoidance when various objects, whether stationary or moving, are considered in the formulation.

2.6 Hybrid System Design

Collision avoidance can assume more than just one type of evasive maneuver. That is, depending on the type of threat and state of the system, collision avoidance could have several very different schemes. The idea of platooning in an automated highway system is the close packing of a group of vehicles separated from other groups by a substantial distance. There is much writing concerning interplatoon and intraplatoon distances, joining and splitting platoons, coordinating platoons among traffic, and lateral and longitudinal controllers for platoons [17][18]. These ideas are based on the fact that collisions are less severe with lesser relative velocities. Moreover, even with platooning traffic density is kept high. Platooning poses two main types of collisions: those amongst platoons and those between platoons. The collision avoidance systems for these two types might be significantly different.

An entire collision avoidance scheme may incorporate many of the aforementioned schemes into one system, with the end result as a hybrid system. For example, far away, a collision avoidance system might utilize non-cooperative game theory techniques in order to optimize avoidance, but this may not provide a sufficient separation after some time, and a more cooperative technique is needed. Of course, this assumes the threat is actually a friendly and both are connected to a centralized unit. [21] discusses a combined non-cooperative and cooperative strategies for decentralized control and centralized control, respectively; ultimately leading to a hybrid system.

The ideas behind fuzzy neural networks may indicate that solutions to collision avoidance problems may not be obtainable in closed-form or may be too difficult to calculate. Hybrid systems take advantage of the discrete and continuous nature of systems in order to classify problems into a continuous and discrete state space analyzed for reachable and invariant sets. Hybrid techniques may also be applied to a single collision avoidance system. Controlled invariant sets and reachable sets for a non-cooperative approach are detailed in [19]. Behind a given system its algorithm might not be semi-decidable. Fortunately, in practice, we are interested in finite time computations rather than computing out to negative infinity. This will allow approximations but still will render a successful collision avoidance system.

2.7 Motivation and Future Intentions for FLASH Vehicle

Whereas the following analysis using game-theory will have certain unrealistic assumptions, and in fact, some of the designed controllers will likely not be directly implemented, an actual system could incorporate game theory. This could be done by removing assumptions and thus including other variables pertinent to the examined system. However, the main drive of this paper is to figure ways to keep the simplicity of the system with assumptions, e.g., a hybrid technique could be employed to retain these properties. Nonetheless, a game-theoretic approach is superior and worth devotion as its

flexibility and mathematically representative of a worst-case scenario, which for collision avoidance is a high priority. Moreover, this approach easily extrapolates to other pursuit-evasion systems involving airplanes, missiles, ships, etc.

The ideas in this paper will be redirected to the FLASH vehicle in hopes of future work and assessment of this paper in simulation and trials on a scaled highway.

Chapter 3
Modeling and Solution Forms

3.1 Mathematical Model

3.1.1 FLASH Kinematic Model

Whereas the bulk of this thesis will utilize the "rolling disc" model in an effort to leave much extrapolation available to non-automobile collision avoidance, the nonholonomic model has a unique construction and is worth mentioning for its ability to model a front-wheel turning type vehicle. The resulting path-following model will also become important in real space and in building the cost function in Chapter 5. The car has two basic inputs: its velocity and steering. Practically, both inputs will be bounded by a lower and upper value; thus, the input space will be a compact space.

Nonholonomic constraints dictate that there is no velocity component normal to the direction of the rolling wheel. For small steering angles, the vehicle may be accurately modeled as a bicycle where the weight and position of the vehicle are assumed to be located at the middle of the rear-axle. Refer to Figure 3.1.

The position and orientation of the car can be described by four variables. Figure 3.1 shows each of these variables. The coordinates (x, y) give the location of the center of the rear axle. The car's angle with respect to the x-axis is given by θ. Let ϕ denote the steering wheel angle with respect to the car's longitudinal axis. Thus the velocity of the car is given by:

$$\dot{x} = v_1 \cos\theta$$
$$\dot{y} = v_1 \sin\theta$$

v_1 is the linear velocity of the rear wheels. l is the length of the vehicle. The velocity components of the front axle become functions of the rear axle and can be written similarly.

Assuming neither slippage nor perpendicular velocity components means the velocities of the front and rear axles have angles with respect to the x-axis the same as the angles of rolling direction. This implies

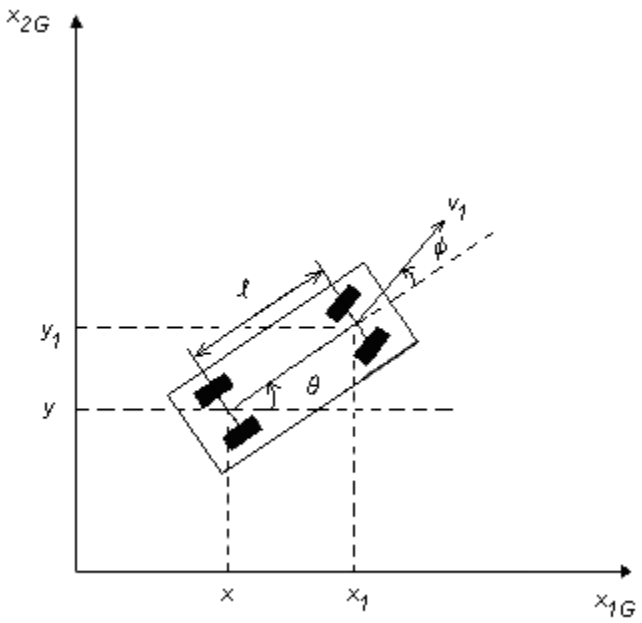

Figure 3.1: Global coordinate system for robotic vehicle [9]

$$\dot{x}\sin(\theta+\phi) = \dot{y}\cos(\theta+\phi) \tag{3.1a}$$

$$\dot{x}_1\sin(\theta+\phi) = \dot{y}_1\cos(\theta+\phi) \tag{3.1b}$$

Plugging in velocity components in (3.1) results in an equation for $\dot{\theta}$, and thus the kinematic model is given by

$$\begin{bmatrix}\dot{x}\\ \dot{y}\\ \dot{\theta}\\ \dot{\phi}\end{bmatrix} = \begin{bmatrix}\cos\theta\\ \sin\theta\\ \dfrac{\tan\phi}{l}\\ 0\end{bmatrix} v_1 + \begin{bmatrix}0\\ 0\\ 0\\ 1\end{bmatrix} v_2 \tag{3.2}$$

where v_2 is the angular velocity of the front wheels. Due to sensor measurements, local variables are preferred over global variables. The global variables can be expressed in more path-relative state variables as

$$\begin{bmatrix}\dot{s}\\ \dot{d}_1\\ \dot{\theta}_p\\ \dot{\phi}\end{bmatrix} = \begin{bmatrix}\dfrac{\cos\theta_p}{1-d_1c}\\ \tan\theta_p\\ \dfrac{\tan\phi}{l} - \dfrac{c\cos\theta_p}{1-d_1c}\\ 0\end{bmatrix} v_1 + \begin{bmatrix}0\\ 0\\ 0\\ 1\end{bmatrix} v_2 \tag{3.3}$$

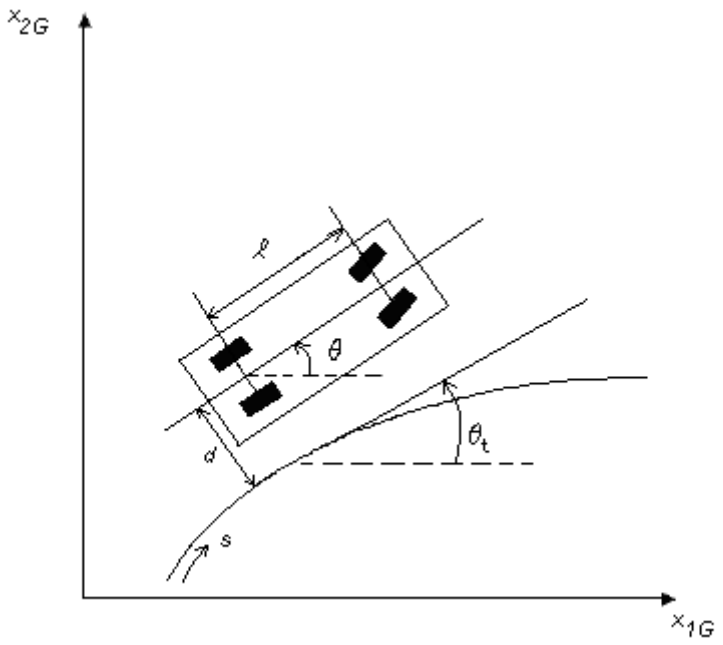

Figure 3.2: Path following coordinate system for robotic vehicle [9]

where d_1 is the positive or negative distance of a line perpendicular to the axle, extending from the rear axle's midpoint to a point on the path, s is arc length, $\theta_p = \theta - \theta_t$, and $c(s)$ is the path's curvature given by $\frac{d\theta_t}{ds}$, where θ_t is the angle of the tangent line to the x-axis where the line is formed perpendicular to the car's longitudinal axis going through the rear axle's midpoint. These parameters are depicted in Figure 3.2.

3.1.2 Abstracting to Rolling Disc

In normal mode, collision avoidance will be unnecessary and the model of the vehicle would be better treated with nonholonomic constraints and certain lateral controllers may be used, such as in [5] or [9]. In order to ease the mathematical manipulation, and to keep the dimension of the problem small, (3.2) will be abstracted to a "rolling disc", which is a simpler model, yet can match any trajectory given by (3.2). Moreover, local accessibility, or controllability, is maintained as a mapping exists which translates this property. This mapping should be able to show that the rolling disc model is implementable by the bicycle model, that is, for all trajectories possible by the rolling disc, there exists a corresponding trajectory by the bicycle with respect to some smooth

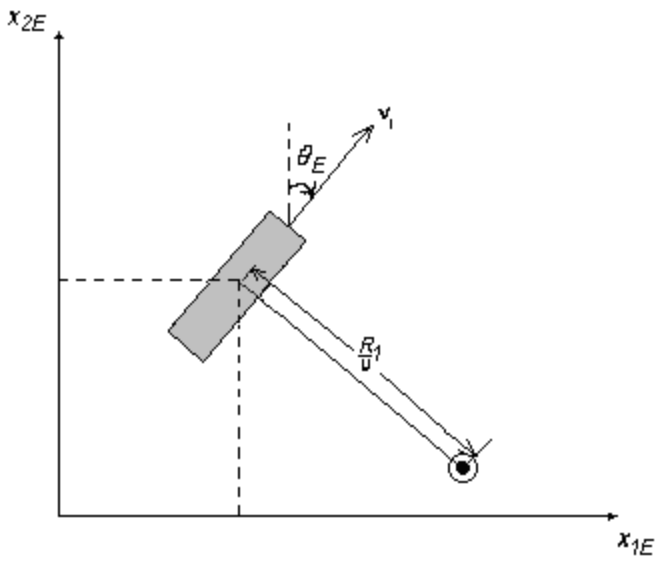

Figure 3.3: Global coordinate system and parameters for rolling disc model

map. This is possible if the rolling disc did not have zero linear velocity, or in essence could not rotate at a fixed point. Obviously the car cannot turn the steering wheel 90° to the left or right since with perfect traction the car would not move at all. However, the car could follow a circular path about this fixed point an arbitrarily small distance approximating the rolling disc rotation. In our model for the car, the velocity will be fixed and non-zero. In our model for the moving object, if the velocity is measured as zero, then we will assume the object is not rotating, which for collision avoidance does not make a difference.

The kinematic model of the vehicle may be dropped one dimension by excluding the length of the car (or essentially the ϕ parameter) and assuming the car as a point mass moving with some bounded velocity and bounded angular velocity. This vehicular model is one in which it selects at each instant a value for the velocity and a value for the curvature.

$$\dot{x}_{1E} = v_1 \sin\theta_E \tag{3.4a}$$
$$\dot{x}_{2E} = v_1 \cos\theta_E \tag{3.4b}$$
$$\dot{\theta}_E = \omega_1 u \tag{3.4c}$$

where the subscript 'E' refers to E, v_1 is a constant linear velocity, ω_1 is the evader's maximum angular velocity, and u is a piecewise continuous function representing the selection of curvature, with the constraint $u \in [-1,1]$. Note the equations are referenced from the global coordinate frame (x_{1E}, x_{2E}) with θ_E as the angle subtended clockwise

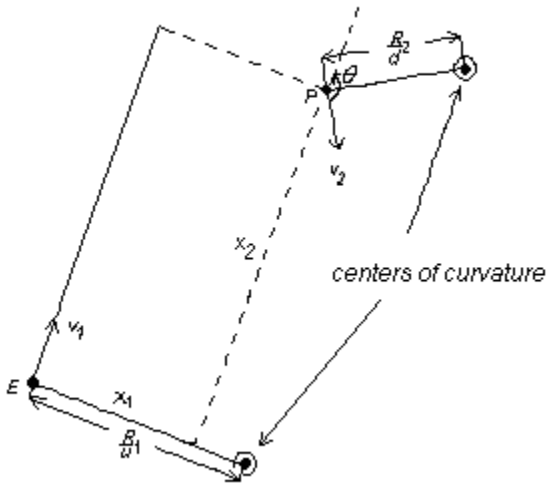

Figure 3.4: Relative coordinate frame from E's (vehicle's) point of view

from the vertical axis. Also the minimum turning radius for the vehicle is $R_1 = \frac{v_1}{\omega_1}$. Thus the normalized curvature selection u determines a curvature of $\frac{u}{R_1}$, or a turning radius of $\frac{R_1}{u}$. See Figure 3.3.

It will be assumed the vehicle is equipped with sensors in order to detect the colliding object's maximum linear velocity and maximum angular velocity in order to cast it into a model structured the same as the vehicle itself. These bounds are realistic in the sense if P is not another vehicle, such as a deer, it is unlikely P will be able to instantaneously move in any direction, like backwards. Thus the model for P in the same global coordinate frame (x_{1E}, x_{2E}) follows similarly:

$$\dot{x}_{1P} = v_2 \sin\theta_P \tag{3.5a}$$
$$\dot{x}_{1P} = v_2 \sin\theta_P \tag{3.5b}$$
$$\dot{\theta}_P = \omega_2 d \tag{3.5c}$$

where the 'P' subscript refers to P, v_1 is the linear velocity, ω_1 is the maximum angular velocity, and d is a piecewise continuous, with the constraint $d \in [-1,1]$. A relative model is more appealing and can reduce the state equations to three dimensions, (x_1, x_2) as the coordinates of P with respect to the E, and θ as the relative heading. The positive

x_2-axis is aligned with E's velocity vector and so θ is defined as the angle of P's velocity vector subtended clockwise from the vertical axis. See Figure 3.4. The dynamics can now be described as

$$\dot{x}_1 = -\omega_1 u x_2 + v_2 \sin\theta \tag{3.6a}$$
$$\dot{x}_2 = -v_1 + \omega_1 u x_1 + v_2 \cos\theta \tag{3.6b}$$
$$\dot{\theta} = \omega_2 d - \omega_1 u \tag{3.6c}$$

where $u \in [-1,1]$ and $d \in [-1,1]$. This model is classically known as the "two cars model". Note this model may include stationary objects (e.g. boulders, road kill, etc.) by allowing $v_2 = 0$.

3.2 Using Differential Game

We assume the collision avoidance scenario involves our vehicle and some other object. Note this object may include another vehicle, an animal, or stationary object, all of which may not cooperate. For example, another driver may lose control or is just not paying attention. Cooperation of any type would only benefit the correct driver in allowing a further separation from this unsafe set. Thus this analysis considers a worst-case maneuver which encompasses all theoretical threats according to the two models.

For these reasons, collision avoidance is treated as a game of two players with the vehicle as an evader (E) and some potential threat as a pursuer (P). It may or may not be known whether the threat is fully aware of the vehicle as the vehicle is aware of the threat. Through appropriate sensors the vehicle could collect past and present locations of P. In order to be prepared for the worst case scenario, it is then assumed that the threat knows its opponent's, the vehicle's, motion. Thus, we analyze a non-cooperative game in which E attempts to maximize an index and avoid collision while the second attempts to minimize this same index and pursue collision. A cooperative game, which may appeal to collision avoidance systems among vehicles through a centralized control unit, can be formulated by replacing the min-max operation with a max-max operation.

3.3 Cost Formulation

The process (3.13) is to be run using a performance measure of the form

$$J(x(t),t,\underset{t\le s\le t_f}{u(s)},\underset{t\le s\le t_f}{d(s)}) = l(x(t_f),t_f) + \int_t^{t_f} L(x(s),u(s),d(s),s)ds \tag{3.7}$$

where player 1's input is u, player 2's input is d, $l : R^n \times R \to R$ is a differentiable function characterizing the terminal constraint of the problem, and $L : R^n \times R \times R \times R \to R$ is a function characterizing a Lagrangian running cost. Notice J has been left time-varying and a functional over the input signals $u(\cdot) \in U$ and $d(\cdot) \in D$ where

$$U \equiv \{\eta_1 : [t, t_f] \to [-1,1] \mid \eta_1(\cdot) \text{ is measurable}\}$$
$$D \equiv \{\eta_2 : [t, t_f] \to [-1,1] \mid \eta_2(\cdot) \text{ is measurable}\}$$

which are input strategy spaces both over the compact space $[-1,1]$ where each strategy is a measurable function. We shall refer to back to the general form when we consider different selections in Chapter 5, but until then we refer to a simpler terminal cost.

An important safety measure with which the evader and pursuer are maximizing and minimizing, respectively, is their Euclidean distance. In games, this can be expressed as a terminal constraint,

$$J(x, t, u(\cdot), d(\cdot)) = l(x(t_f)) \tag{3.8a}$$
$$l(x) = \sqrt{x_1^{\,2} + x_2^{\,2}} - \kappa \tag{3.8b}$$

where κ is the radius of a circular region centered around E within which a collision has taken place. So, $l(x)$ denotes the distance from a collision event. This is needed for analysis and of course since E takes up physical space. Although a vehicle is more box-shaped than circular, this will ease the mathematics. Looking at (3.8b), we see that

$$T = \{x \in R^n : l(x) \le 0\} \tag{3.9}$$

is a target volume for P, i.e., if $l(x) \le 0$, then P is either on or inside the collision circle. We initially define t_f as the time at which T is penetrated:

$$t_f = \inf\{t \in R^+ : x(t) \in \operatorname{int} T\} \tag{3.10}$$

The boundary of T, ∂T, described by $l(x) = 0$, in the three dimensional space can be represented as a cylinder in $\theta \in [0, 2\pi]$.

3.4 Hamiltonian Formulation

As long as the cost formulation, J is separable in u and d, the compact region $[-1,1]$ guarantee a saddle solution, i.e., there exists $u^*(\cdot) \in U$ (resp. $d^*(\cdot) \in D$) which

maximizes (resp. minimizes) the performance measure J over the strategy space U (resp. D). Denoting these operations mathematically, the optimal controls are given as

$$u^*(t) = \arg\max_{u(\cdot)\in U} J(x,t,u(\cdot),d(\cdot)) \tag{3.12a}$$

$$d^*(t) = \arg\min_{d(\cdot)\in D} J(x,t,u(\cdot),d(\cdot)) \tag{3.12b}$$

Define the Hamiltonian,

$$H(x,p) = L(x,u,d) + p \cdot f(x,u,d) \tag{3.13}$$

where p is the co-state (adjoint) vector also defined as $p^T(t) = V_x(x(t),t)$. Hamilton's set of $2n$ equations become:

$$\dot{x}^* = \frac{\partial H}{\partial p}(x^*, p^*) = f(x^*, u^*, d^*) \tag{3.14a}$$

$$\dot{p}^* = -\frac{\partial H}{\partial x}(x^*, p^*) \tag{3.14b}$$

So, the co-state equations for an optimal trajectory $x^*(t)$ for the terminal cost problem are

$$\begin{aligned} \dot{p}_1{}^* &= -\omega_1 u^* p_2{}^* \\ \dot{p}_2{}^* &= \omega_1 u^* p_1{}^* \\ \dot{p}_3{}^* &= v_2(p_2{}^* \sin\theta^* - p_1{}^* \cos\theta^*) \end{aligned} \tag{3.14b}$$

where p_i represents the ith component of the co-state. Let $\phi(t_f)$ represent the angle subtended clockwise from the x_2-axis of the location of P at termination. $p(t_f)$ points toward the greatest increase in the cost function so it must point outward from the capture cylinder, or more precisely,

$$\begin{aligned} p_1(t_f) &= \sin\phi(t_f) \\ p_2(t_f) &= \cos\phi(t_f) \\ p_3(t_f) &= 0 \end{aligned} \tag{3.14c}$$

We define the value function as the optimization of the cost function, i.e.,

$$V = \max_{u(\cdot)\in U} \min_{d(\cdot)\in D} J(x,t,u(\cdot),d(\cdot)) \tag{3.15}$$

It does not matter whether the 'min' operation is applied first or the 'max' operation is applied first since each f_i and L are separable in u and d, i.e., there are no cross-terms (e.g. ud). If V is smooth, then V satisfies the Hamilton-Jacobi-Isaacs (HJI) equation:

$$V_t + H^o(x, V_x) = 0 \tag{3.16}$$

with boundary condition $V(x, t_f) = l(x(t_f))$ and where $H^o(x, V_x) = \max_{u \in [-1,1]} \min_{d \in [-1,1]} H(x, p)$ is the optimized Hamiltonian.

3.5 General Form of Controls

Consider the optimal Hamiltonian in the game with a terminal cost,

$$H^*(x, V_x) = \max_{u \in [-1,1]} \min_{d \in [-1,1]} [-\omega_1 u A + v_2 (V_1 \sin\theta + V_2 \cos\theta) - V_2 v_1 + V_3 \omega_2 d] = 0$$

with $A = x_1 V_2 - x_2 V_1 - V_3$. The Hamiltonian is set to zero since the value of the game does not explicitly depend on time. Further explanation will be given later, though it is not needed here. The optimal controls for u and d become

$$u^* = \operatorname{sgn} A \tag{3.22a}$$
$$d^* = -\operatorname{sgn} V_3 \tag{3.22b}$$

3.6 Analytic Solution and PDE Characteristics

3.6.1 Analytic Solution

We look for solutions V of the Hamilton-Jacobi-Isaacs partial differential equation (HJI PDE)

$$V_t + H^o(x, V_x) = 0$$

where V will soon be constructed as a collection of characteristics in smooth regions and later as a viscosity solution in non-smooth regions. In smooth regions, back propagation of equilibrium trajectories will be started from near miss terminal points on the capture cylinder and will help determine the level set $V = 0$ and other values of V. Similar to Merz's paper on the game of two identical vehicles [27], we classify only three types of retrograde equilibrium trajectories and give their explicit solutions. The reasons for only

three and their significance in the formation of the barrier will become clearer in Chapter 4 and 5. Back propagation is arbitrarily assumed to begin at $\tau = 0$ from the capture cylinder.

Type 1: $u = -d = \pm 1$

$$x_1 = \kappa \sin(\phi_0 + \omega_1 u\tau) + R_1 u(1 - \cos\omega_1 u\tau) - R_2 u[\cos(\theta_0 + \omega_1 u\tau) - \cos\theta] \quad (3.23a)$$

$$x_2 = \kappa \cos(\phi_0 + \omega_1 u\tau) + R_1 u \sin\omega_1 u\tau + R_2 u[\sin(\theta_0 + \omega_1 u\tau) - \sin\theta] \quad (3.23b)$$

$$\theta = \theta_0 + u(\omega_1 + \omega_2)\tau \quad (3.23c)$$

Type 2: $u = d = \pm 1$

$$x_1 = \kappa \sin(\phi_0 + \omega_1 u\tau) + R_1 u(1 - \cos\omega_1 u\tau) + R_2 u[\cos(\theta_0 + \omega_1 u\tau) - \cos\theta] \quad (3.24a)$$

$$x_2 = \kappa \cos(\phi_0 + \omega_1 u\tau) + R_1 u \sin\omega_1 u\tau - R_2 u[\sin(\theta_0 + \omega_1 u\tau) - \sin\theta] \quad (3.24b)$$

$$\theta = \theta_0 + u(\omega_1 - \omega_2)\tau \quad (3.24c)$$

Type 3: $u = \pm 1, d = 0$

$$x_1 = \kappa \sin(\phi_0 + \omega_1 u\tau) + R_1 u(1 - \cos\omega_1 u\tau) - v_2 \tau \sin\theta \quad (3.25a)$$

$$x_2 = \kappa \cos(\phi_0 + \omega_1 u\tau) + R_1 u \sin\omega_1 u\tau - v_2 \tau \cos\theta \quad (3.25b)$$

$$\theta = \theta_0 + \omega_1 u\tau \quad (3.25c)$$

These equations with their constant inputs can be shown to satisfy the relative kinematic equations (3.6).

3.6.2 Method of Characteristics

With a time-varying value function, the HJI PDE has characteristics with normal $\xi \in R^4$, where the dimension has been increased by one in treating the time variable as a new state, i.e., $x_4 = t$, and the above PDE can be rewritten as:

$$V_4 + \max_{u\in[-1,1]} \min_{d\in[-1,1]} \{L + V_1 f_1 + V_2 f_2 + V_3 f_3\} = 0$$

where $V_i = \dfrac{\partial V}{\partial x_i}$ and f_i is the i$^{\text{th}}$ component of the velocity of the trajectory. The characteristic equation of this PDE can be found once a value for E's input and the disturbance are selected. The characteristics of the HJI equation transmit underlying system's dynamics through optimal trajectories, and for a game with only a terminal cost, the terminal conditions are transmitted. So if $\zeta_f(\cdot, x, t, d(\cdot), u(\cdot))$ is an optimal trajectory

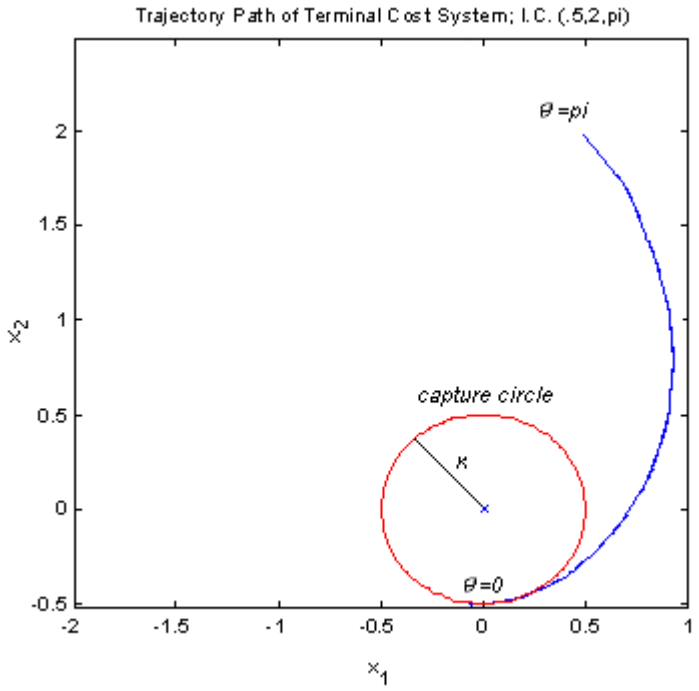

Figure 3.5: Merz's trajectory of type 1; initial condition on barrier

of the HJI,

$$V(x,t) = V(\zeta_f(0;x,t,d(\cdot),u(\cdot)),0)$$

for all time $t \le 0$ for a valid solution $V(x,t)$. This makes sense for the solution since for any new initial condition on the equilibrium, as long as u and d continue to behave optimally, the trajectory will hit the same terminal location on the capture cylinder; thus achieving the same V. We shall use the method of characteristics to prove this mathematically for the case when $V(x,t)$ is smooth.

Proof:

Consider a nonlinear 1st order PDE of the form:

$$a(x,y,V)V_x + b(x,y,V)V_y - c(x,y,V) = 0 \qquad (3.26)$$

where x and y are independent variables for V, i.e., $V = V(x,y)$. x denotes the state while y could denote a time variable. We define $I(x,y,z) \equiv V(x,y) - z \equiv 0$ so that the solution $V(x,y)$ can be represented as a surface in (x,y,z) coordinate system when $I = 0$.

Since $I = 0$ identically, $\dot{I} = 0$, or

$$\frac{\partial I}{\partial x}\dot{x} + \frac{\partial I}{\partial y}\dot{y} + \frac{\partial I}{\partial z}\dot{z} = 0, \text{ or}$$

$$V_x\dot{x} + V_y\dot{y} - \dot{z} = 0$$

Comparing this latter equation to (3.26), we immediately see

$$\dot{x} = a(x, y, V) \tag{3.27a}$$
$$\dot{y} = b(x, y, V) \tag{3.27b}$$
$$\dot{z} = c(x, y, V) \tag{3.27c}$$

This is the method of characteristics, and with an initial condition, the system of ordinary differential equations describe the evolution of $V(x, y)$ over (x, y) where $V(x, y)$ is assumed smooth. Applying this to a terminal cost system, if we let $y = t$ and x be the states, the PDE

$$V_t + V_x f(x, u^*, d^*) = 0$$

transforms into

$$\dot{x}^* = f(x^*, u^*, d^*) \tag{3.28a}$$
$$\dot{t} = 1 \tag{3.28b}$$
$$\dot{V} = 0 \tag{3.28c}$$

since $z = V(x, t)$ and where $u^*(\cdot) \in U$ and $d^*(\cdot) \in D$ are optimal strategies depending on the initial condition of the system. Thus, if $V(x, t)$ is a smooth solution, it remains constant over a characteristic of the system. []

3.6.3 Main Equation

We assume a value function exists, V is time-invariant or the time variable has been included in the state, i.e. $V = V(x)$, and $V \in C^1(\Omega)$ on some domain Ω. Then from equation (3.13), V satisfies

$$H^o = \max_{u \in [-1,1]} \min_{d \in [-1,1]} \{L + V_x \cdot f(x, u, d)\} = 0 \tag{3.29}$$

The latter equation of (3.29) is referred to as the "main equation". Its derivation, e.g. found in [32] is based on a Taylor series expansion of the type

$$\int_t^{t+h} g(x)dx = hg(t) + \frac{1}{2}h^2 g'(t+\lambda h),$$

where $g(x)$ is some function, $\lambda \in (0,1)$, and h is small, and is also based on defining a small vector $e = (e_1,...,e_n)$ such that $e_j = f_j(x,u,d)h$, representing a small displacement in x. Since L or V is assumed "autonomous", i.e., not explicit functions of time, then the main equation can also be seen as a result of the constancy of the Hamiltonian Condition, or Second Erdmann Condition [24]. The constant becomes zero since a small change in V corresponds to an opposite signed integral of the running cost over a short period h. However, a zero constant may also appear in the time-varying case. From the main equation, it is observed $\dot{V} = V_x \cdot f(x^*,u^*,d^*)$ along any optimal path. This implies $\dot{V} = 0$ for a terminal cost formulation or V remains constant along an optimal path. This is the same result produced by the method of characteristics. In general, $\dot{V} = -L(x^*,u^*,d^*)$.

3.6.4 Classical Derivation and Relevance of the HJI PDE

A value function is constructed as the optimization of a cost function. Many derivations of a HJ PDE are readily available from many optimal control theory books [24][25][29]. We shall consider the single player optimization problem, which may be easily extended to the 2 player case. So consider the problem $(Q_{t,x})$:

$$(Q_{t,x})\begin{cases} Minimize \rightarrow \int_t^T L(s,q(s),\dot{q}(s))ds + g(q(T)) \\ q(t) = x \end{cases} \tag{3.30}$$

over Lipschitz continuous functions q where L and g are the running and terminal costs, respectively.

For this setup, we can describe the HJ as

$$(\text{HJ})\begin{cases} q_t(t,x) + \min_{\dot{q}\in R^n}\{q_x(t,x)\cdot\dot{q} + L(t,q,\dot{q})\} = 0 \\ q(T,x) = g(x) \end{cases} \tag{3.31}$$

for all $t \in (S,T)$ and $q \in R^n$.

Define the value function $V:[S,T]\times R^n \to R$ such that $V(t,x)=\inf(Q_{t,x})$, where 'inf' denotes the infimum cost of the problem $(Q_{t,x})$. This denotes the optimal cost when the trajectory begins at space x and time t. Then if V is continuously differentiable and if for each $(t,x)\in[S,T]\times R^n$, the optimization problem has a minimizer $\overline{q}$ which is also continuously differentiable, then V is a solution to the corresponding HJ equation.

This implies that if one could determine a family of continuously differentiable minimizers $\{q_{t,x}\}$, one could select

$$q(t,x)=\int_t^T L(t,q_{t,x}(s),\dot{q}_{t,x}(s))ds+g(q_{t,x}(T)) \tag{3.32}$$

and if q turned out to be continuously differentiable, then $V=q$ and q would be the desired HJ solution.

This construction of a field of extremals is similar to the method of characteristics in their building of solutions from an initial line of data. However, Hamiltonian's set of $2n$ equations describes a different set of ordinary differential equations (ODE's).

The converse, in which an optimal control problem can be solved through finding a solution to the HJE, results from Hamilton's equation being necessary conditions. We will further analyze the HJI PDE and Hamilton's equations and their relationship to help set guidelines for solving the differential game when different costs are used.

3.6.5 When Value Function is Not Differentiable

Classical solutions may not exist if shocks and rarefactions are present in any Hamilton-Jacobi equation. Since in general the value function is not differentiable, along characteristics of the HJI will be found shocks and rarefactions. Shocks are discontinuities in the value function V as a function of the states x and are points of intersection of retrograde trajectories with different optimal inputs. These points are also known as dispersal points, and fall along lines on the barrier and on surfaces inside the barrier. Rarefactions are points where different retrograde trajectories are possible as a result of multiple optimal inputs at these points. In the game with a terminal cost, the possible trajectories from rarefactions all must have the same value V since the non-retrograde trajectories meet at this point. Generalized solutions are introduced to characterize the solution amidst shocks, while numerical techniques are introduced to plot the barrier around these points. These are explored in Chapter 6.

Looking at the optimal control strategies (3.22), u^* and d^* remain constant along a characteristic until the terms in the switch functions change signs or become zero. This

will be shown to occur in (3.22b) whenever a retrograde trajectory breaks from a singular line or surface. At that point, u^* or d^* may switch to a nonsingular value but the trajectory still runs along essentially the same characteristic. The reason for this is the breaking time has no effect on the terminal condition since these trajectories all lead to the same singular line or surface and then to the same terminal condition.

The adjoints become discontinuous whenever a retrograde trajectory reaches a dispersal line. Beyond this line, the controls (3.22) are no longer optimal and in fact, it signifies the end of the retrograde trajectory, or the initial condition of this barrier trajectory.

Chapter 4

Safe and Unsafe Sets

This chapter covers the details and meaning behind optimal trajectories which result in a collision, "near miss", or miss as delivered in a differential game setup. The terminal cost setup in Chapter 3 allows us to analyze paths where ultimately all that we care about is that a collision is avoided. It in essence provides a framework with which may shape collision avoidance mathematically and assess possible control strategies a priori.

4.1 Defining Safe and Unsafe

Using the terminal cost (3.8), we consider a "game of kind", one in which we distinguish a finite number of cases: safe, unsafe, or nearly safe. This is directly related to the sign of J, i.e., these cases occur when respectively $J > 0$, $J = 0$, or $J < 0$ (i.e., respectively, $l(x(t_f)) > 0$, $l(x(t_f)) = 0$, or $l(x(t_f)) < 0$). In the state space, we already know that T encloses unsafe points since if $x \in \text{int}\, T$, a collision has already occurred. For the most part, for given parameters v_1, v_2, ω_1, and ω_2, there are initial locations and orientations of P outside the capture cylinder which will guarantee avoidance under our differential game approach. This will allow for correctly assuming that there are two distinguishable sets: a "safe" set and an "unsafe" set. The former consists of trajectories where no matter what P does, as long as E behaves optimally, theoretically a miss is guaranteed, whereas the latter consists of trajectories where there is a potential for a collision, despite what E does. In fact, a collision is guaranteed as long as P behaves optimally. There might exist holes in the "barrier" between the unsafe and safe set such that P could potentially drive the trajectory out of the safe set. However, we will note that this usually occurs with only a faster and more maneuverable pursuer, which we would like to believe, is not the case.

4.2 Trajectories in Safe and Unsafe Sets

The vehicle's interest lies in the safe set, denoted as S_1. S_1 is the largest subset of $R^n \setminus T$ which can be rendered invariant, i.e., with the terminal cost (3.8), for any moves made by P there exists a play by the vehicle E which keeps $J \geq 0$. So

$$S_1 = \left\{ x \in R^3 \setminus T : \exists u(t) \in U, J(x,t,u(t),d^*(t)) \geq 0 \right\} \tag{4.1}$$

This is the space within which E is assured safety despite any maneuvers made by P. Inside S_1, the vehicle may play any control, which is commonly referred to as a least restrictive law. If the trajectory reaches the boundary, however, then the vehicle must consider playing optimally lest the trajectory crosses into the unsafe set, $\overline{S}_1 = R^3 \setminus S_1$. We will soon look at safe trajectories for E and what E may do before it must act decisively.

As mentioned before, optimal trajectories under (3.8) will have the same value V for any given point on that path since they all lead to the same terminal condition. In the analysis where we consider near misses under optimal play, or the cases when $V = 0$ (dealt with in detail in Chapter 5), these trajectories form a "barrier" dividing the safe and unsafe set in which optimal trajectories lead to misses or collisions, respectively. This barrier analysis is referred to as the game of kind analysis; since once the analysis is complete, we have enough information to decide if a miss, near miss, or collision has occurred.

We consider an optimal trajectory to lie in the unsafe set if after a finite amount of time, x has reached $\operatorname{int} T$ So $\overline{S}_1$ can be better formulated as

$$\overline{S}_1 = \left\{ x \in R^3 : V(x, -\infty) < 0 \right\} \tag{4.2}$$

Note P has as much time as it needs to cause a collision. But for our analysis, we will devote more time to $v_1 > v_2$ than $v_2 > v_1$ since we would like to neglect cases where P could eventually catch up to E (like a heat-seeking missile). We will soon look at unsafe trajectories and what E may do to decrease the chances or even the impact of a possible collision.

With a terminal constraint, it is natural to first look at the terminal conditions of the problem.

4.3 Near-Miss Terminal Conditions

The capture cylinder is first divided into a usable part (UP) and a non-usable part (NUP) separated by what is known as the boundary of the usable part (BUP). We will cover these topics as a gateway to Chapter 5 and as a basic framework integral to a game-theoretic approach.

4.3.1 Boundary of the Usable Part

The boundary of the usable part (BUP) corresponds to the terminal points of near miss trajectories which meet the capture circle tangentially, and also marks the beginning of the barrier. Along the BUP, P cannot force a collision and E cannot force a miss, since each player has a control to counter the other. These trajectories realistically represent situations where P can just miss E on either the left or right side of E, respectively.

The BUP can be represented mathematically by assuming both players play optimally at termination:

$$\max_{u\in[-1,1]} \min_{d\in[-1,1]} \upsilon^T f(x,u,d) = 0 \tag{4.3}$$

where υ is a vector normal to ∂T, i.e.,

$$\upsilon = \frac{\partial l}{\partial x}(x(t_f))$$

In order to find the BUP for our particular kinematic setup, we first parameterize T as:

$$x_{10} = \kappa \sin\phi_0$$
$$x_{20} = \kappa \cos\phi_0$$

with

$$\phi_0 \in [0,2\pi]$$
$$\theta_0 \in [0,2\pi]$$

where we have set $t_f = 0$ for convenience, the subscript '0' refers to this terminal time, and ϕ_0 is the terminal angle defined earlier in Chapter 3. Note that in [28], ϕ_0 is subtended counterclockwise. This is changed in order to ease the parameterization in the case of non-identical vehicles. From (3.19), and noting that $\upsilon_1 = \sin\phi_0$, $\upsilon_2 = \cos\phi_0$, and $\upsilon_3 = 0$, (essentially the normal to the capture cylinder),

$$\max_{u\in[-1,1]} \min_{d\in[-1,1]} \upsilon^T f(x,u,d) = v_2(\sin\theta_0 \sin\phi_0 + \cos\theta_0 \cos\phi_0) - v_1 \cos\phi_0 = 0$$

where the terms multiplying $\omega_1 u$ sum to zero. Rearranging,

$$\sin\phi_0(v_2 \sin\theta_0) - \cos\phi_0(v_1 - v_2 \cos\theta_0) = 0$$

This gives a parameterization of the BUP for the angle ϕ_0 as a function of θ_0. Let $W = \sqrt{v_1^2 + v_2^2 - 2v_1 v_2 \cos\theta_0}$. Then the BUP is completely parameterized by:

$$\sin\phi_0 = \pm\frac{v_1 - v_2\cos\theta_0}{W} \tag{4.4a}$$

$$\cos\phi_0 = \pm\frac{v_2\sin\theta_0}{W} \tag{4.4b}$$

The $\pm$ indicates the BUP consists of a pair of diametrically opposite points for a given θ_0. W is like a normalizing factor which keeps the right hand side of (4.4a)-(b) within the interval $[-1,1]$. So we may also express terminal points along the BUP,

$$x_{10} = \pm\frac{\kappa(v_1 - v_2\cos\theta_0)}{W} \tag{4.5a}$$

$$x_{20} = \pm\frac{\kappa v_2\sin\theta_0}{W} \tag{4.5b}$$

4.3.2 Properties at BUP

The BUP holds the final state condition for the boundary of the safe and unsafe sets, S_1 and $\overline{S}_1$. On ∂T, the optimal Hamiltonian loses dependency on the optimal controls since $A = 0$ and $V_3 = 0$ as seen by plugging in the parameterization of T. The final values for the optimal controls are found indirectly through the retrograde derivatives of A and V_3, which if evaluated on ∂T at termination, imply either A and V_3 grow positively or negatively as the trajectory retrogresses from the capture cylinder. This idea will be utilized later in this chapter and the next. Nonetheless, optimal control(s) for E and P along the BUP can be determined. It will be shown in the next chapter that the BUP is broken up into few segments where u^* and d^* are constant(s).

4.4 Steady-State Techniques

[22] uses similar analytic trajectory types as those stated in Chapter 3 but for the case of identical vehicles, and then uses level set techniques combined with retrogression to construct a representation of the steady state unsafe set in the game of kind.

If there are no discontinuities in $V(x,t)$ as a function of x, then a steady state solution must annul the HJI equation (3.16), or satisfy our main equation (3.29). That is, $H^o(x,V_x)=0$. Then in the game of kind, the gradient V_x remains normal to the velocity vector $f(x,u^*,d^*)$. Thus along the boundary of the safe and unsafe set at $t=0$, i.e., BUP, as it is propagated back in time, this condition must remain true. What this means is the greatest increase in the value function, or the direction E would like to force the trajectory, is oriented towards the safe set and perpendicular to the barrier. E "pushes" in this direction in anticipation of the trajectory missing the capture cylinder, but since P "pushes" in the opposite direction, the trajectory rides along the barrier. Keeping these necessary conditions, [22] retrogresses these trajectories out to infinity (actually some number) forming a zero level set, i.e., a set bounded by $V=0$. This set is the unsafe set.

We will mirror some of the techniques of [22] in the case of non-identical vehicles. We will consider slices of constant θ and setup the mathematics and iterations needed to generate the left and right barriers in this constant plane. Note there is a left and right barrier as retrogressed from the left and right BUP. Also note the left and right barrier in the constant plane will be two lines; and for $v_1 > v_2$ will likely intersect at a crossover point since the entire left and right barriers will likely divide the state space into safe and unsafe sets. There may be instances where they do not and it will be necessary to exclude the leak in the barrier for this θ. As mentioned before, we would like to exclude fancy maneuvering through the barrier under optimal play.

Other methods which may not fully utilize the analytic solutions but could handle a non-terminal cost formulation may include polyhedral approximations, Taylor series expansions, or fast marching methods [40][41]. [40] devises a technique which encompasses power series method of Al'brecht about a point, projects retrogressive extremals using the Pontryagin Principle off of boundaries of the point's neighborhood, and then develops ordinary differential equations for possible higher partial derivatives in these neighboring extremals. The process may be repeated throughout a grid. [40] focuses toward the Hamilton-Jacobi-Bellman PDE equation, but it could be extended to the HJI PDE and would be a topic for future research. The power of this technique lies in its ability to handle higher dimensions without "the curse of dimensionality". This will become important as we will see adjusting costs and adding variables increases dimension and the analytic techniques are lost.

4.5 Game Inside and Outside Barrier

To consider other possible trajectories than those analyzed in Chapter 5, we briefly look at the cases when P is initially located inside or outside the barrier, but not on it. The formulation for the inside is known as the game of degree, and techniques will be similar to those of the game of kind. The formulation for the outside must be slightly adjusted in order to have a termination time.

4.5.1 Game Outside

4.5.1.1 Closest Point of Approach

If an optimal trajectory lies outside the barrier, then the terminal time as defined in (3.10) will become infinite since P never reaches the interior of the capture cylinder. So consider $r^2 = x_1^{\,2} + x_2^{\,2}$ and when the derivative of r, reaches zero:

$$\dot{r} = \frac{x_1\dot{x}_1 + x_2\dot{x}_2}{\sqrt{x_1^{\,2} + x_2^{\,2}}} \equiv 0 \quad \Rightarrow \quad x_1\dot{x}_1 + x_2\dot{x}_2 = 0 \tag{4.6}$$

We redefine

$$t_f = \inf\{t_0 < 0 : x_1(t_0)\dot{x}_1(t_0) + x_2(t_0)\dot{x}_2(t_0) = 0\} \tag{4.7}$$

This occurs at the closest point of approach for outside barrier trajectories, indicating a miss has occurred. Terminal conditions may also be rewritten as

$$x_0 = \begin{bmatrix} r_0 \sin\phi_0 \\ r_0 \cos\phi_0 \\ \theta_0 \end{bmatrix} \tag{4.8}$$

Plugging (4.8) in (4.6)

$$\Rightarrow \quad x_1(-\omega_1 u x_2 + v_2 \sin\theta) + x_2(-v_1 + \omega_1 u x_1 + v_2 \cos\theta) = 0$$

$$\Rightarrow \quad v_2 r_0 \cos(\theta_0 - \phi_0) - v_1 r_0 \cos\phi_0 = 0$$

$$\Rightarrow \quad \frac{v_2}{v_1} = \frac{\cos\phi_0}{\cos(\theta_0 - \phi_0)} \tag{4.8}$$

If the vehicle wanted to know the closest point of approach, it could do this by monitoring ϕ_0 and θ_0 until the above equality is satisfied and then verifies it is the minimum, perhaps through a second order condition. However, E could also detect this point through perpetual sensing of P.

4.5.1.2 Controls

With a terminal point at some $r_0 > \kappa$, we can retrogress optimal trajectories if we knew the optimal controls. In the game of kind, we note the terminal co-state points outward from the capture cylinder and again A and p_3 are both zero. But without going into more details, the results would be the same as if the radius of the capture cylinder was instead r_0. Thus optimal trajectories retrogressed from this terminal miss distance would travel along a new "barrier" encompassing the old barrier, $r_0 = \kappa$.

One could do this if a buffer zone is desired for any optimal play by P. However, this is no new information other than supposing the vehicle is "bigger" in a sense. Practically, the vehicle may want to implement a different controller than this as it may dart off the road when an object arrives in its sensors' range. As mentioned before, E may play any control until the trajectory, if at all, reaches the actual barrier at which point E should switch to the optimal control to be assured of collision avoidance.

Practically again, the vehicle may want to anticipate a possible situation by choosing a suboptimal steering angle. This could be done in several manners. For example, from forming several "barriers" with several different $r_0's > \kappa$, depending on which "barrier" and the portion of that "barrier" the initial condition is closest to, one could replace the original optimal control dictated by that barrier with a suboptimal one. That is, if we had two encompassing "barriers" representing $r_0 = 1.5\kappa$ and $r_0 = 2\kappa$, we could replace their $u^* = 1$ portions with $u^* = .8$ and $u^* = .5$, respectively. In this case the farther P lies away, the less E turns. Nonetheless E is turning and chances will be less that the trajectory reaches the real barrier than if E hadn't turn at all using the least restrictive law.

Another method might be to move out of the game of kind and utilize a running cost. Unless one uses time to termination or separating distance as a running cost, the optimal controls will likely be less extreme. But one could incorporate secondary objectives other than collision avoidance. This might include reduced turning, gas expenditure, braking, or deviation from a nominal path. Although one may have to introduce more dimensions to the problem, and we will see that the analytic solutions are lost, the formulation is built into one cost and continuous, unlike the hybrid type solution presented in the previous paragraph. We shall later introduce some simple running costs depicting these ideas.

4.5.2 Game Inside

The inside barrier analysis is commonly replaced with a game of degree in which the players seek the best procedure in optimizing some continuous payoff. Despite the fact

that terminal conditions represent collision, we adopt a payoff which might be beneficial to E such as the time to termination.

$$J(x,t,u(\cdot),d(\cdot)) = \int_{t}^{0} ds \tag{4.9}$$

If E cannot avoid collision, then it might attempt to delay this occurrence in hopes that P plays non-optimally, perhaps avoiding collision. Similarly in this game, P hopes to collide as quickly as possible. Otherwise, a game of kind analysis would leave E with any control as the optimal one and this would not be any added information. Fortunately, this particular payoff is one in which a terminal cost may be "maintained" and analysis can proceed with the analytic solutions we obtained in the game of kind. Moreover, since there is a high potential for collision, we will continue with this particular payoff in order to provide the vehicle with the safest maneuvers.

A terminal cost formulation still indicates the terminal optimal controls as the co-state points continues to point in a direction with the greatest increase in the value function, i.e., normal to the capture cylinder. Thus as we retrogress optimal trajectories, E plays away from P and P plays towards E. Thus we expect these trajectories to be equivalent in nature to the game of kind trajectories on the barrier.

4.5.2.1 Usable Part

The UP is the set of points on ∂T such that P may force penetration into T. Thus, under optimal play, termination will only immediately occur at the UP (and of course within T). So, the UP is such that for any input u, there exist a disturbance d^* where $f(x,u,d^*)$ has a component in the direction opposite to υ, thus pushing the trajectory into the cylindrical region, i.e.,

$$\min_{d\in[-1,1]} \upsilon^T f(x,u,d^*) < 0 \tag{4.10}$$

for all $u \in [-1,1]$. The UP is essentially that part of the capture cylinder where P can force a collision. For example, if the speed of P was always less than the speed of the E, i.e., $v_1 > v_2$, then the UP would be located mostly in the positive x_2 territory of the cylinder since in this case most collisions would occur towards the front or front-side of E.

4.5.2.2 Dispersal Surface and Universal Surface

We will briefly setup the termination of two important singular surfaces, which will be seen to be similar to the singularities in the game of kind. We do this to illustrate their meaning at termination and what they reveal in the state space.

4.5.2.3 Dispersal Surface for E

The co-state dynamics (3.14b) and necessary optimal controls (3.22) are still valid. Moreover, we already noted the boundary conditions to the co-states are the same. The terminal controls, however, must be reconsidered since they will, like in the game of kind, be undefined. Let x_0 be a terminal point on the UP, where

$$x_0 = \begin{bmatrix} \kappa \sin\phi_0 \\ \kappa \cos\phi_0 \\ \theta_0 \end{bmatrix}$$

Likewise,

$$p_0 = \begin{bmatrix} \sin\phi_0 \\ \cos\phi_0 \\ 0 \end{bmatrix}$$

Again, since the switch functions have zero arguments at termination, we look towards their retrograde derivatives. At termination,

$$\overset{o}{A} = -v_1 \sin\phi_0 \quad \Rightarrow \quad u = -1 \quad \text{for } x_{10} > 0 \tag{4.11a}$$

$$\Rightarrow \quad u = 1 \quad \text{for } x_{10} < 0 \tag{4.11b}$$

Note we are only considering terminal angles ϕ_0 which lie in between the left and right BUP. One angle $\phi_0 = 0$, which for all of its points are included on the UP when $v_1 > v_2$, must be further considered since $\overset{o}{A} = 0$. So we look toward the 2nd retrograde derivative:

$$\begin{aligned} \overset{oo}{A} &= -v_1 \omega_1 u p_{20} \\ &= -v_1 \omega_1 u \cos\phi_0 \\ &= -v_1 \omega_1 u \end{aligned}$$

So, $u = -\operatorname{sgn} u$, or

$$\Rightarrow \qquad u = 0 \qquad \text{for } x_{10} = 0 \tag{4.11c}$$

At first this seems unsettling. The only time we want E to be heading straight is if P is directly behind E and heading in the same direction, but we will find this to be the terminal line for a dispersal surface (DS) and thus no equilibrium solution end here. That is, the formation of the DS requires neighboring trajectories when $u = -1$ and $u = 1$.

Suppose $\theta_2 = \pi$ and P is initially on the x_2-axis within the unsafe set, i.e., P and E are initially heading towards each other. Then by symmetry, E may elect to turn either full left or right with the same time to collision under optimal play. The DS can be constructed similarly to a dispersal line (DL) which will be found in the barrier formation in the next chapter. They represent points where multiple optimal trajectories may emanate with the same cost. In a game of degree, these are paths with the same time to collision, i.e., $\tau_2 = \tau_2'$, where we use the notation from the DL construction in Section 5.4. If for all points on the DS in a given θ_2, the types of both paths are known, then they may be equated and a dispersal point locus (x_1, x_2) as function of (θ, τ) can be found. The DS will be seen to intersect the capture cylinder at the line represented by $(x_1, x_2) = (0, \kappa)$. As we know these paths are generated from either side of this line, the DS splits E's control, i.e., $u = -1$ on one side and $u = 1$ on the other.

4.5.2.4 Universal Surface for P

Similarly, the terminal controls for P may be found similarly through the retrograde derivatives of p_3. At termination,

$$\overset{o}{p}_3 = v_2 \sin(\phi_0 - \theta_0) \quad \Rightarrow \quad d = -1 \qquad \text{for } \theta_0 < \phi_0 \text{ or } \theta_0 > \phi_0 + \pi \tag{4.12a}$$

$$\Rightarrow \quad d = 1 \qquad \text{for } \phi_0 < \theta_0 < \phi_0 + \pi \tag{4.12b}$$

Note again we are only considering those $\theta_0 \in [0, 2\pi]$ and $\phi_0 \in [0, 2\pi]$ combinations which lie on the UP on the capture cylinder. Basically the lines $\theta_0 = \phi_0$ and $\theta_0 = \phi_0 + \pi$ are diametrically opposing lines which wrap around the capture cylinder splitting it into two equal regions, one of which representing $d = -1$ and the other $d = 1$. These regions intersected with the UP (e.g., if $v_1 > v_2$, the UP is roughly the top portion of the capture cylinder and thus there will be two lines of singularities in P's control), denote the collision regions in which the optimal control for d is given by the corresponding extreme.

We must again looks towards the second retrograde derivative to find the terminal controls here

$$\overset{oo}{p}_3 = \omega_2 d \cos(\phi_0 - \theta_0)$$

which implies

$$d = -\operatorname{sgn} d \quad \text{for } \theta_0 = \phi_0$$
$$d = \operatorname{sgn} d \quad \text{for } \theta_0 = \phi_0 + \pi$$

$$\Rightarrow \quad d = 0 \quad \text{for } \theta_0 = \phi_0 \tag{4.12c}$$
$$\Rightarrow \quad d = 0, \pm 1 \quad \text{for } \theta_0 = \phi_0 + \pi \tag{4.12d}$$

The multiple solutions for $\theta_0 = \phi_0 + \pi$ and singular control for $\theta_0 = \phi_0$ indicate the end of two universal surfaces (US) inside the unsafe set when $v_1 > v_2$. Like a universal line (UL) found in the barrier formation in the next chapter, a universal surface (US) represent points where multiple trajectories may meet. Here lie trajectories where P is heading straight. For any initial condition within the unsafe set, if P acts optimally, its strategy is to orient itself to E's minimum turning circle and if time remains heads straight to collide minimizing the time to collision.

The US's intersection with any θ can be found by eliminating θ_0 in the type 3 trajectory equations, i.e., $\theta_0 = \theta - \omega_1 u \tau$ and plugging this into the remaining two equations. The resulting line (x_1, x_2) as a function of (θ, τ) describes the US between the capture circle and the DS or between the capture circle and the barrier.

4.5.2.5 Singular Surfaces Complete Unsafe Game

The US's and DS partition the unsafe set into regions where the optimal controls will be seen to be constant, and the constants are given by the determination of the terminal controls. The constancy of controls will be looked at in more detail with respect to the barrier of the safe and unsafe set. Thus, these surfaces make the game inside the unsafe set known according to a game with time to termination as the payoff.

Chapter 5

Barrier Formation in Game of Kind

This chapter discusses the formation and techniques used to construct the barrier and its singular lines in the game of kind with the variable parameters v_1, v_2, ω_1, and ω_2. It will become commonplace for us to refer to the game of identical vehicles, in which $v_1 = v_2$ and $\omega_1 = \omega_2$. Since this analysis was originally done in [27], we shall refer to the normalized case, i.e., $v_1 = v_2 = \omega_1 = \omega_2 = 1$ as Merz's parameters.

The barrier will be investigated in using terminal strategies and analytic representations for all points on the barrier, with the exception of crossover points, which will be set up numerically. This chapter is a brief overview and introduction to the next two chapters.

5.1 BUP

5.1.1 Parameterization of BUP

We must make a distinction as to whether $v_1 > v_2$ or $v_2 > v_1$. For $v_2 > v_1$, $\sin\phi_0$ changes sign when $\cos\phi_0 = \frac{v_1}{v_2}$. This implies the UP spirals around the capture cylinder. The BUP parameterization was found earlier to be

$$x_{10} = \pm\frac{\kappa(v_1 - v_2\cos\theta_0)}{W} \tag{5.1a}$$

$$x_{20} = \pm\frac{\kappa v_2 \sin\theta_0}{W} \tag{5.1b}$$

where again the '-' refers to the "left" side BUP and the '+' refers to the "right" side BUP. We denote in this manner since for $v_1 > v_2$, the BUP comprises two sinusoidal lines each located separately and diametrically on either side of the capture cylinder. See Figure 5.1 for a rough sketch, and note the "left" and "right" BUP are in the direction of $x_1 < 0$ and $x_1 > 0$, respectively.

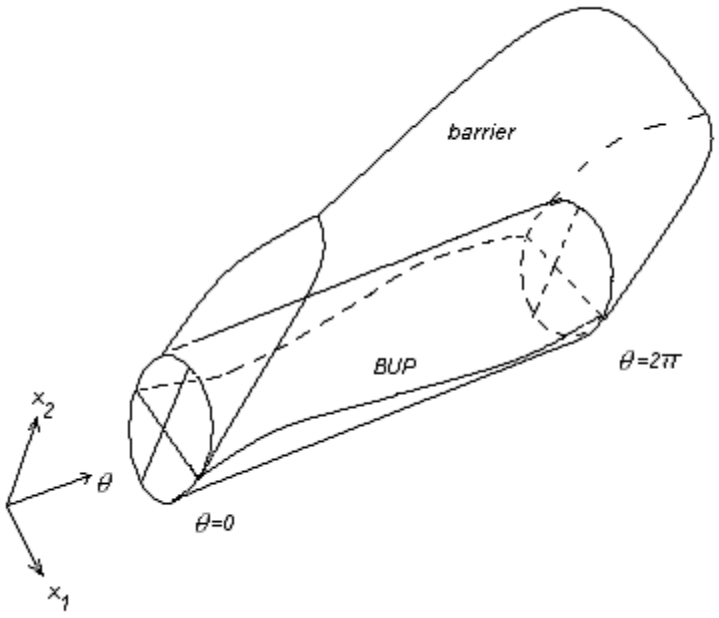

Figure 5.1: 3-D Picture of capture cylinder, BUP, barrier (rough). $v_1 > v_2$.

The UP is the region in which $f(x,u^*,d^*)$ has a component in the direction of the capture cylinder; i.e., a normal vector $\upsilon = (0,1,0)$ at the point $x = (0,\kappa,0)$ indicates

$$\begin{aligned}\max_{u\in[-1,1]}\min_{d\in[-1,1]}\upsilon\cdot f &= \max_{u\in[-1,1]}\min_{d\in[-1,1]}[-v_1+\omega_1 u x_1+v_2\cos\theta]\\ &= -v_1+v_2\\ &< 0\end{aligned}$$

so the UP is the area which includes the top portion of the capture cylinder bounded by the left and right BUP. This was mentioned in the previous chapter and now we have verification. See Figure 5.1.

Now assume $v_2 > v_1$. Let s_2 be the angle in the 1st quadrant such that $\cos s_2 = \frac{v_1}{v_2}$. Thus at $\theta_0 = s_2$ and $\theta_0 = 2\pi - s_2$, x_1 changes sign for either the left '-' or right '+' barrier. For the right barrier, the BUP has an x_1-component which follows a negative cosine function offset by a constant. So the x_1-component is negative from $\theta_0 = 0$ to $\theta_0 = s_2$, positive from $\theta_0 = s_2$ to $\theta_0 = 2\pi - s_2$, and then negative from $\theta_0 = 2\pi - s_2$ to $\theta_0 = 2\pi$. Similarly, the x_2-component follows a positive sine function and so is positive from $\theta_0 = 0$ to $\theta_0 = \pi$, and then negative from $\theta_0 = \pi$ to $\theta_0 = 2\pi$. As a result the BUP is a

sinusoid curve from $x=(0,-\kappa,0)$ to $x=(0,\kappa,\pi)$ to $x=(0,-\kappa,2\pi)$. The "left" BUP is the diametrically opposing curve.

For the case $v_1=v_2$, $\theta_0=\cos^{-1}\left(\frac{1}{1}\right)=0$, and x_{10} and x_{20} become undefined. The case with which Merz [27] considers, i.e., $v_1=v_2=\omega_1=\omega_2=1$, will become an important example, and so we look again at the BUP equation (3.20) to derive a parameterization. Without going through the details, the BUP becomes parameterized as

$$\theta_0=0 \qquad \text{or} \qquad \theta_0=2\phi_0 \tag{5.2ab}$$

Thus the parameterization is the capture circle $\theta_0=0$ and two straight lines of which the right BUP joins $(0,\kappa,0)$ and $(0,-\kappa,2\pi)$ and the left BUP is diametrically opposite to the right.

The UP in Merz's game begins as a semicircle in the negative x_2 direction at $\theta_0=0$, then as θ_0 approaches 2π the UP spirals around the cylindrical axis clockwise rotating a full 2π radians. Notice that changes in v_1 and v_2 only affect the expansion or shrinking in the θ direction and not stretching of the BUP around the capture cylinder.

As mentioned before, we will mainly consider the $v_1>v_2$ case.

5.1.2 Terminal Strategies along BUP

It is seen that $A=0$ and $V_3=0$ at termination along the BUP. But looking at the retrograde time derivative at termination,

$$\begin{aligned}\overset{o}{A} &= (\omega_1 u x_2 - v_2\sin\theta)V_2 + x_1(-\omega_1 u V_1) - (v_1-\omega_1 u x_1 - v_2\cos\theta)V_1 - x_2(\omega_1 u V_2) \\ &\qquad + v_2(V_2\sin\theta - V_1\cos\theta) \\ &= -v_1 V_1 \\ &= -v_1\sin\phi_0 \end{aligned} \tag{5.3}$$

the sign of $\overset{o}{A}$ shows locally the sign of A as the trajectory pulls away from the capture cylinder. This implies at termination

$$u = -\operatorname{sgn}\left(\pm \frac{v_1 - v_2 \cos\theta_0}{W} \right)$$
$$= \mp 1 \tag{5.4}$$

since $v_1 > v_2$. So on right BUP, $u = -1$ and on left BUP, $u = 1$.

$$\overset{o}{V}_3 = v_2 \left(V_1 \cos\theta - V_2 \sin\theta \right)$$
$$= v_2 \left(\pm \frac{v_1 - v_2 \cos\theta_0}{W} \cos\theta_0 \mp \frac{v_2 \sin\theta_0}{W} \sin\theta_0 \right)$$
$$= v_2 \left(\pm \frac{v_1 \cos\theta_0 - v_2}{W} \right) \tag{5.5}$$

which since $d = -\operatorname{sgn} V_3$ implies $d = \operatorname{sgn}(\pm(v_2 - v_1 \cos\theta_0))$

d changes sign depending on the value of θ_0. Let S be the angle in the 1st quadrant such that $\cos S = \frac{v_2}{v_1}$ and let's consider the right BUP. So at termination,

$d = -1$ for $\theta_0 \in [0, S]$ (5.6a)

$= 1$ for $\theta_0 \in [S, 2\pi - S]$ (5.6b)

$= -1$ for $\theta_0 \in [2\pi - S, 2\pi]$ (5.6c)

since the cosine function is even about π. For the left BUP follows quickly

$d = 1$ for $\theta_0 \in [0, S]$ (5.7a)

$= -1$ for $\theta_0 \in [S, 2\pi - S]$ (5.7b)

$= 1$ for $\theta_0 \in [2\pi - S, 2\pi]$ (5.7c)

5.2 UL and DL Terminal Points

Note $\overset{o}{x}_1$ and $\overset{o}{x}_2$ do not depend on d but $\overset{o}{\theta}$ does so it changes abruptly when d switches extremes. Moving along the right BUP in the positive θ_0 direction, as θ_0 passes through S, $\overset{o}{\theta}$ drops by $2\omega_2$. As θ_0 passes through $2\pi - S$, $\overset{o}{\theta}$ jumps up by $2\omega_2$. This means the backward time trajectories from either side of S intersect as τ progresses, forming a dispersal line (DL). Conversely, the backward time trajectories from either side of $2\pi - S$ split apart from one another as τ progresses, leaving a void, indicating a universal line (UL) and its tributary paths.

One of the two BUP points, $\theta_0 = 2\pi - S$ on the right barrier or $\theta_0 = S$ on the left barrier, is the important termination point for any trajectory reaching a UL. We will find their locations useful, so we determine their x_1 and x_2 components. First consider the right barrier:

$$x_{10} = \frac{\kappa(v_1 - v_2 \cos\theta_0)}{W} = \frac{\kappa(v_1 - \frac{{v_2}^2}{v_1})}{\sqrt{{v_1}^2 - {v_2}^2}} = \frac{\kappa\sqrt{{v_1}^2 - {v_2}^2}}{v_1} \tag{5.8a}$$

$$x_{20} = \frac{\kappa v_2 \sin\theta_0}{W} = \frac{-\kappa\frac{{v_2}^2}{v_1}}{\sqrt{{v_1}^2 - {v_2}^2}} = \frac{-\kappa v_2}{v_1} \tag{5.8b}$$

The left barrier point can be found similarly or through symmetry to be

$$x_{10} = \frac{-\kappa\sqrt{{v_1}^2 - {v_2}^2}}{v_1} \tag{5.9a}$$

$$x_{20} = \frac{-\kappa v_2}{v_1} \tag{5.9b}$$

In this thesis we will not consider possible collisions from the rear but they may represent important scenarios on curved roads. This can be further explained through the relationship of the UL with the BUP. Suppose $v_1 > v_2$ and we consider the left barrier. We know the terminal conditions imply P is not only heading straight but also at an angle towards E such that there is a near miss.

For the case $v_1 > v_2$, note $p_{20} < 0$ at the terminal points of the universal lines indicating a near miss at some point behind E, i.e., $x_{20} < 0$. So if the vehicle is traveling down a straight road, these terminal points indicate the vehicle has turned a significant angle if P was initially in front of E. We would like to label these occurrences as unlikely on a straight road, as there are usually lane bounds to consider (treated in Chapter 5), but on curvy roads, pursuers from the side could utilize this strategy. Nonetheless, we will consider initial conditions leading to one of the universal lines in order to illustrate a crossover point.

In Merz's game, the universal lines on the left and right barrier terminate at the same point $(0,-\kappa,0)$ but they are distinct lines. In fact, there are five other valid optimal trajectories which terminate at this point.

5.3 Equilibrium Trajectories

Combining the retrograde solutions with terminal controls will be sufficient to construct the barrier and switching lines for both players. This conclusion is in part a direct result of the definition of the reachable set (refer to Section 3.4) since for points on the boundary of the reachable set, equilibrium strategies must be played by both players, otherwise if P (respectively, E) plays non-optimally while the other, E (respectively P) plays optimally, the resulting trajectory will lie outside (inside, respectively) the reachable set.

The switch arguments in (3.22) are continuous function in x and p, so the barrier consists of regions where the inputs are constants depending on the sign of both switch arguments. Moreover, equilibrium trajectories on the barrier are confined to these regions since any given retrograde equilibrium trajectory ends on a DL or EDL and begins from a UL or the BUP itself. So, equilibrium strategies along the barrier are always constant, with the exception of those trajectories which reach a UL and in that case, P's strategy comprises two constants. This can also be verified by consideration of example trajectories leading from the barrier. Thus, we may integrate retrogressively with constant strategies until a desired switching time τ_1, if along a UL, is achieved which may assume a range of values from zero. Breaking from a UL at this switching time we may choose either $d = 1$ or $d = -1$, and continue retrogressively with this constant strategy.

5.3.1 Barrier Trajectories

So in order to construct the barrier we must locate initial conditions such that under optimal play, the trajectory terminates at the BUP. But it is more effective to use the already determined terminal conditions on the BUP and as before form retrogressive trajectories under optimal play back to these barrier points. Looking at an example, it is clear that these trajectories will be limited to either one or two segments of the three types already mentioned.

5.3.1.1 Crossover Points

Suppose the system begins with the initial condition $\theta_2 = \pi$, $x_1 = 0$ and $x_2 > 0$, i.e., P and E, are initially heading towards each other. This is a shock location, or a dispersal point, since E has the option to choose either full left or right turn ($u = \pm 1$) without a difference in V. It seems for some x_2 the initial condition, whether P assume a singular control or not, are such that P can nearly miss E, or the trajectory terminates on the BUP. Any trajectory with an initial condition where x_2 is greater than this will result in

termination outside the capture cylinder. This x_2 value presents a crossover point, where a left and right barrier trajectory intersect. Whereas the value V is the same for both the left and right trajectories, the terminal locations and the times to termination may or may not be the same. Practically it might be advantageous for the vehicle to choose the route with the greater time-to-go since it is more unlikely P will behave optimally for a greater span of time.

.1 Crossover Trajectory Types

With Merz's parameters, the two crossover trajectories from a given $\theta = \theta_2$ each may exhibit two types of behaviors. The crossover trajectory representing the left barrier may exhibit behavior of type L1 or L2, while the crossover trajectory representing the right barrier may exhibit behavior of type R1 or R2. These crossover types are described below according to their constituent types, retrograde switching times, τ_1 or τ_1' , and times-to-go, τ_2 or τ_2':

L1: type 3 for $\tau \in [0, \tau_1]$, type 1 for $\tau \in [\tau_1, \tau_2]$
R1: type 3 for $\tau \in [0, \tau_1']$, type 1 for $\tau \in [\tau_1', \tau_2']$
L2: type 1 for $\tau \in [\tau_1, \tau_2]$
R2: type 3 for $\tau \in [0, \tau_1']$, type 2 for $\tau \in [\tau_1', \tau_2']$

[27] does not mention how to select which one of the two apply for a given $\theta = \theta_2$, but [28] confirms that it is sufficient to apply a trial and error approach, checking the conditions:

Left Barrier		Right Barrier	
$\tau_1 \le \tau_2$	or	$\tau_1' \le \tau_2'$	(5.10a)
$\tau_1 \ge 0$	or	$\tau_1' \ge 0$	(5.10b)
$\phi_0 \ge 0$	or	$\phi_0' \ge 0$	(5.10c)

For variable v and ω, it is possible another type similar to L2 consisting also of one segment could be expressed for the right barrier, but this has not been verified yet. The conditions are the same with the exception that (5.10c) is replaced by

$$\theta_0 \in [0, 2\pi] \quad \text{or} \quad \theta_0' \in [0, 2\pi] \qquad (5.10d)$$

.2 Finding the Crossover Point

For any $\theta = \theta_2$, two trajectories will emanate from the crossover point. In fact crossover points mark a line on the barrier known as the evader's dispersal line (EDL). The two trajectories may or may not terminate at the same location on the capture cylinder, but the matter is that they are separate optimal trajectories leading to the BUP and create a shock point. Thus we would expect a sharp ridge where the left and right barriers intersect.

The crossover point for a given $\theta = \theta_2$ can be found by equating the left and right trajectories at their respective times, τ_2 and τ_2', when they reach this θ. A set of two nonlinear equations with these two unknowns are formed. These equations require some numerical root finding algorithm, but accuracy is not lost, and in fact, it is noted in [28] that the algorithm used allows even better accuracy than an iterative PDE solver.

Equations for $\begin{bmatrix} x_1 \\ x_2 \\ \theta \end{bmatrix}_{\tau=\tau_2}$ can be determined as functions of θ_2 and τ_2 after an equation for τ_1, if applicable, is determined by using trajectory type 3 and using the end conditions of this trajectory as the initial conditions for the 2nd segment. For further details refer to [28]. Depending on κ, θ_2, v_1, v_2, ω_1, and ω_2, either L1 or L2 may be matched with R1 or R2 in forming the crossover point.

We will set up the equations for the crossover point for the L1-R1 case, and the results for the other three can be found similarly. L1 is first a type 3 then type 1 retrograde trajectory, corresponding to P turning and then heading straight once reaching a tangential route off E's minimum turning circle. Since this crossover trajectory corresponds to the left barrier, $u = 1$, and we find the final condition of the 1st segment to be

$$\theta(\tau_1) = \theta_0 + \omega_1 \tau_1 \tag{5.11a}$$

$$x_1(\tau_1) = \kappa \sin(\phi_0 + \omega_1 \tau_1) + R_1(1 - \cos \omega_1 \tau_1) - v_2 \tau_1 \sin(\theta_0 + \omega_1 \tau_1) \tag{5.11b}$$

$$x_2(\tau_1) = \kappa \cos(\phi_0 + \omega_1 \tau_1) + R_1 \sin \omega_1 \tau_1 - v_2 \tau_1 \cos(\theta_0 + \omega_1 \tau_1) \tag{5.11c}$$

and the final condition of the 2nd segment to be

$$\theta_2 = \theta_0 + \omega_1 \tau_1 + (\omega_1 + \omega_2)(\tau_2 - \tau_1) \tag{5.12a}$$

$$x_1(\tau_2) = x_1(\tau_1) \cos \omega_1(\tau_2 - \tau_1) + x_2(\tau_1) \sin \omega_1(\tau_2 - \tau_1) + R_1(1 - \cos \omega_1(\tau_2 - \tau_1)).... \\ \ldots - R_2[\cos(\theta_0 + \omega_1 \tau_2) - \cos \theta_2] \tag{5.12b}$$

$$x_2(\tau_2) = x_2(\tau_1) \cos \omega_1(\tau_2 - \tau_1) - x_1(\tau_1) \sin \omega_1(\tau_2 - \tau_1) + R_1 \sin \omega_1(\tau_2 - \tau_1).... \\ \ldots + R_2[\sin(\theta_0 + \omega_1 \tau_2) - \sin \theta_2] \tag{5.12c}$$

where we note $\theta(\tau_2) = \theta_2$ is the selected angle slice and the equations (5.12) become functions of the equations (5.11) since the three types of trajectories are functions of their initial conditions (this can be noticed by expanding out the sine and cosine functions in the type 1 trajectory and generalizing $\kappa \sin\phi_0 \to x_{10}$ and $\kappa \cos\phi_0 \to x_{20}$, where now x_{10} and x_{20} are the initial conditions of the trajectory). Solving for τ_1 in (5.12a), we achieve for L1,

$$\tau_1 = \frac{-\theta_2 + \theta_0 + (\omega_1 + \omega_2)\tau_2}{\omega_2} \tag{5.11}$$

We can substitute this in equations (5.11) and (5.12), and then take (5.11) into (5.12) to arrive at equations for $x_1(\tau_2)$ and $x_2(\tau_2)$ as functions of τ_2. This whole process is repeated for the right crossover trajectory, when $u = -1$. Suppose we denote this trajectory with a prime. We can again arrive at equations for $x_1'(\tau_2')$ and $x_2'(\tau_2')$ as functions of τ_2'. We equate the two states since θ_2 is already known, and solve the two nonlinear equations for τ_2 and τ_2'. As mentioned before, this can be done using any root finding algorithm. Since we do not know if L1-R1 is the correct crossover case for this point, we check the conditions (5.10) on τ_1, τ_2, and θ_0, and then similarly for the right trajectory. If these conditions are met, then the original assumption is correct; otherwise, we must try the remaining three cases. Once a case is found, the crossover point can be found from either trajectory; e.g., from the left, the crossover point would be $(x_1(\tau_2), x_2(\tau_2), \theta_2)$.

.3 Numerical Method for Computing Crossover

Below are snippets of code used in computing the crossover point. The snippet from the function 'crossover' looks at the L1-R1 case, computing the retrograde time for each side, i.e., τ_2 and τ_2'. This is done indirectly through the function 'backtimes' which sets up the equations for the Matlab function 'solve'. This generates the two times τ_2 and τ_2', and from these τ_1 and τ_1' can be computed knowing the crossover point case. The conditions are checked, and if a condition fails, another case is chosen and the process is repeated. Note that these other cases are not shown in the snippets for 'crossover'. Moreover, we only show the L1 case in the snippet for 'crossX1'. The rest is similar. The full code for computing the crossover point is not included in the appendix of this thesis since it hasn't been fully debugged.

```
=========================================================================
function [bcase, params, pos] = crossover(theta2)
% This function locates the crossover point on the barrier for
% theta = theta2.
% inputs-   theta2 = relative angle slice
```

```
%           kappa = capture circle radius
% outputs-  bcase, 2 x 1 vector
%           bcase(1) specifies left trajectory (L1,L2)
%           bcase(2) specifies the right trajectory (R1,R2)
%           pos, 2 x 1 vector, crossover pt.

% Define model parameters for problem
glob_vars

% First assume L1 and R1 trajs
bcase = [1; 1];
tau2 = solve('backtimes',[2; 2],[],[], bcase, theta2);

t2 = tau2(1);
t2p = tau2(2);
t1 = 1/w2*(theta0-theta2+(w1+w2)*t2)
t1p = 1/w2*(-theta0p+theta2+(w1+w2)*t2p)

if((t1 < 0)|(t1 > t2))
  % try case 2 on the left.........

....

  x1 = crossX1(bcase, theta2, 1, t2);
  x2 = crossX2(bcase, theta2, 1, t2);
  pos = [x1; x2];


================================================================================
function g = backtimes(t, bcase, theta2)

%2 = prime = right barrier
%1 = no prime = left barrier

if (bcase(1)==1 & bcase(2)==1)

g(1) = crossX1(bcase,theta2,1,t(1))-crossX1(bcase,theta2,0,t(2));
g(2) = crossX2(bcase,theta2,1,t(1))-crossX2(bcase,theta2,0,t(2));

....


================================================================================
function x1 = crossX1(bcase, theta2, left, t)
%
%    computes the crossover point for the given tau = t
%    for the given crossover case
%    if left = 1 computes the left trajectory, otherwise the right

  if(left)              % left trajectory
     u=1;
    switch bcase(1)
    case 1              % L1 = type 3, type 1
     theta0 = acos(v2/v1);
     x10 = -kappa*sqrt(v1^2-v2^2)/v1;
     x20 = -kappa*v2/v1;
```

```
     W1_t1 = w1/w2*(theta0-theta2+(w1+w2)*t)

     x11 = x10*cos(u*W1_t1) + x20*sin(u*W1_t1) + R1*u*(1-cos(u*W1_t1))
- v2/w1*W1_t1*sin(theta0+u*W1_t1);
     x21 = x20*cos(u*W1_t1) - x10*sin(u*W1_t1) + R1*sin(u*W1_t1)) -
v2/w1*W1_t1*cos(theta0+u*W1_t1);

     x12 = x11*cos(u*(w1*t-W1_t1)) + x21*sin(u*(w1*t-W1_t1)) + R1*u*(1-
cos(u*(w1*t-W1_t1))) - R2*u*(cos(theta0+u*(w1*t-W1_t1)) - cos(theta2));
     ....
```

.4 Example

As an example, assuming $\kappa = .5$ and Merz's parameters, $v_1 = v_2 = \omega_1 = \omega_2 = 1$, we will find the left and right crossover trajectories for $\theta_2 = \pi$, plot both, including their point of intersection. Due to the bugs in the previous program, we devised, and include below, Matlab code focused towards Merz's parameters in finding the two retrograde time parameters, τ_2 and τ_2', and their corresponding switch times, τ_1 and τ_1'. Matlab's Simulink (Figure 5.2) was also used to simulate the trajectories from the initial point to the point of safe contact with the capture cylinder. Figure 5.3 shows the (x_1, x_2) components of the resulting L1 crossover trajectory and Figure 5.4 shows a three-dimensional view of both the L1 and R1 trajectories. Note both L1 and R1 make safe contact at the same terminal condition.

```
=========================================================================
 function crossexample
%Merz crossover point retrograde time computation

[tau2 tau2p] = solve('1-2*cos(t2)-(.5+2*t2-2*3.14+3.14)*sin(t2)+cos(-
3.14) = 2*cos(t2p)-1+(.5+2*t2p-3.14)*sin(t2p)-cos(-3.14)','2*sin(t2)-
(.5+2*t2-2*3.14+3.14)*cos(t2)-sin(-3.14) = 2*sin(t2p)-(.5+2*t2p-
3.14)*cos(t2p)+sin(-3.14)','t2,t2p')
x12 = 1-2*cos(tau2(1))-(.5+2*tau2(1)-2*3.14+3.14)*sin(tau2(1))+cos(-
3.14)
x12p = 2*cos(tau2p(1))-1+(.5+2*tau2p(1)-3.14)*sin(tau2p(1))-cos(-3.14)

x22= 2*sin(tau2(1))-(.5+2*tau2(1)-2*3.14+3.14)*cos(tau2(1))-sin(-3.14)
x22p = 2*sin(tau2p(1))-(.5+2*tau2p(1)-3.14)*cos(tau2p(1))+sin(-3.14)
```

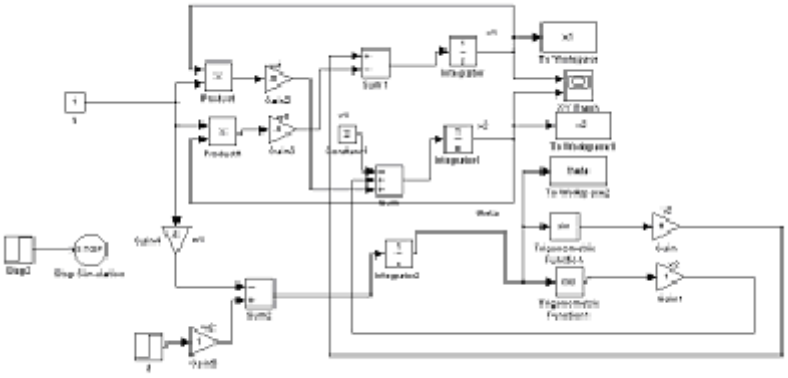

Figure 5.2: Simulink Model of Kinematics (3.6)

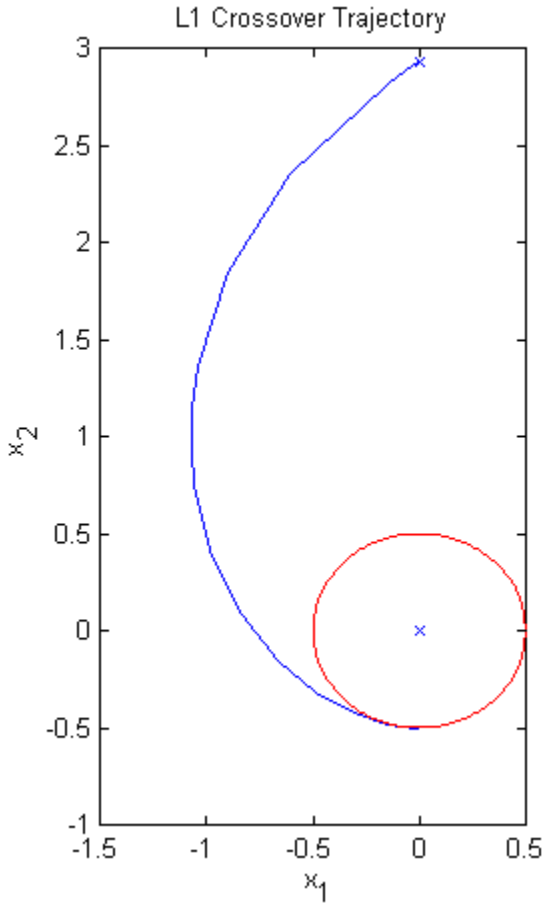

Figure 5.3: Left crossover trajectory; case of identical vehicles ($v_1 = \omega_1 = v_2 = \omega_2 = 1$)

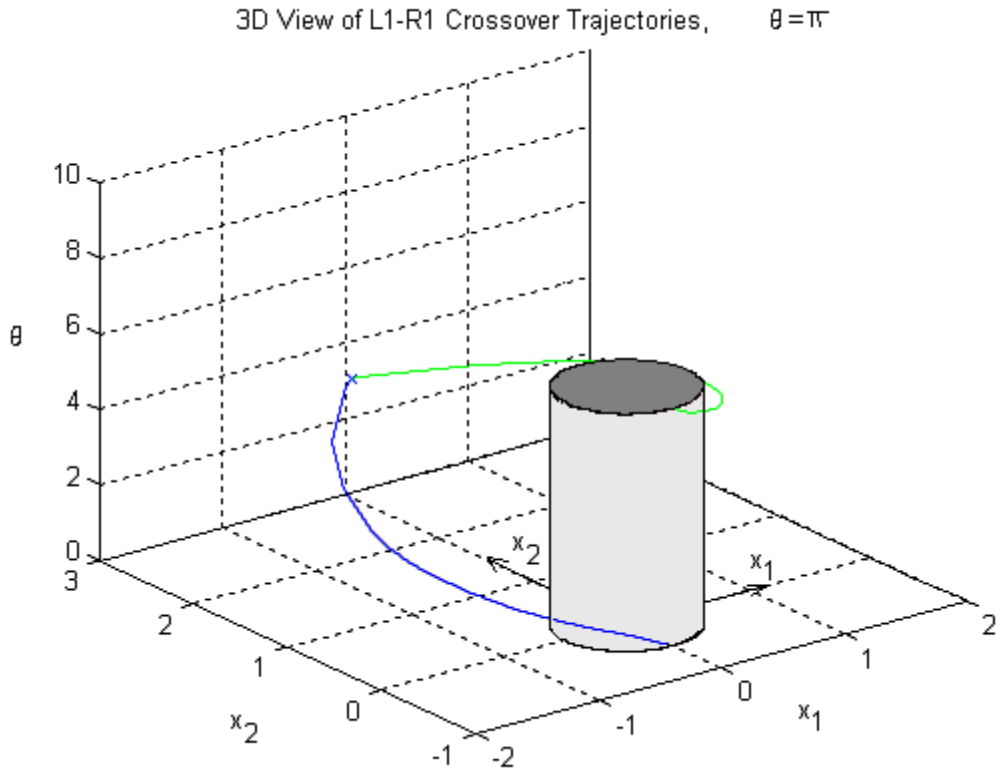

Figure 5.4: Left and right crossover trajectories; case of identical vehicles ($v_1 = \omega_1 = v_2 = \omega_2 = 1$)

.5 Results

It makes sense L1-R1 is the resulting case because for $\theta_2 = \pi$, the maximum possible relative distance between P and E such that P nearly misses E under optimal play could only come from an initial condition where P is some x_2 distance and zero x_1 distance from E. At the point when the switch time reaches zero, there is no travel along the UL and a single type trajectory is taken. For this example, it was found $\tau_1 = 1.64$, $\tau_2 = 2.39$, $\tau_1' = 1.64$, and $\tau_2' = 2.39$, and the crossover point location was found to be $(0, 2.93, \pi)$. The equal time values and x_1 component being zero are a result of the symmetry of the problem.

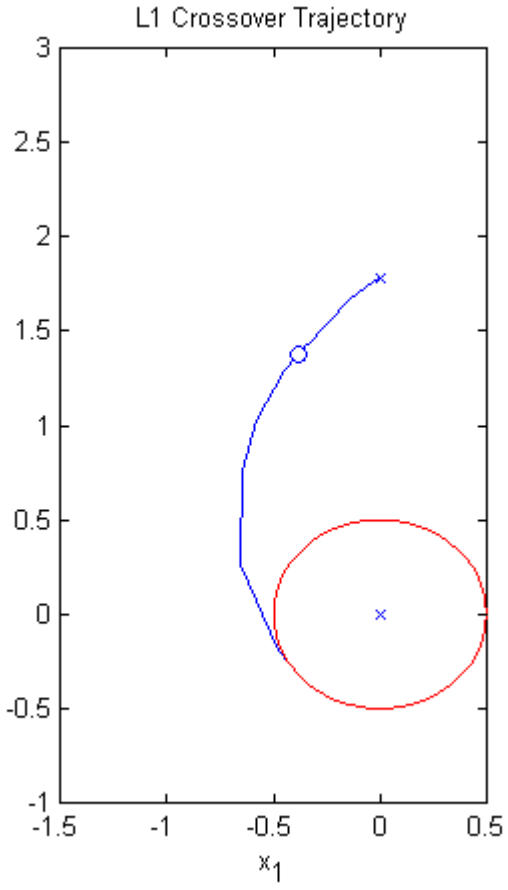

Figure 5.5: Left crossover trajectory; case of non-identical vehicles ($v_1 = 1.5$, $\omega_1 = 2$, $v_2 = 1$, $\omega_2 = 4$)

.6 Comparison

To compare the results in the previous section, we look at $\theta_2 = \pi$, also an L1-R1 trajectory case, when the vehicles are non-identical. We selected $v_1 = 1.5$ and $\omega_1 = 2$ for E and $v_2 = 1$ and $\omega_2 = 4$ for P. Thus, while E is faster, P is able to turn more quickly. Figure 5.4 and Figure 5.5 show the same type of plots as was done for the case of identical vehicles. Also, it was found $\tau_1 = .633$ and $\tau_2 = .805$ and equal values for the right side. The crossover point location was found to be $(0,1.78,\pi)$. Thus, the times-to-go and switching times have been reduced and the crossover location indicates the barrier for this value of θ is smaller than that in the case of identical vehicles. This is of course a result of E's increased speed and P's ability to turn sharper.

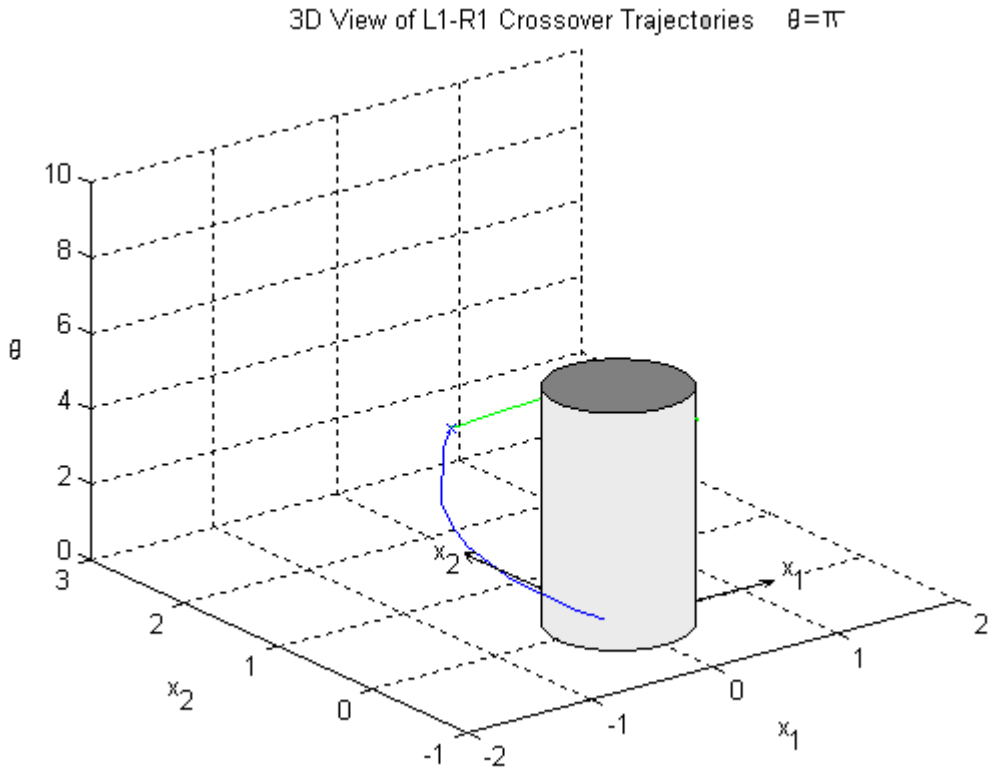

Figure 5.6: Left and right crossover trajectories; case of non-identical vehicles ($v_1 = 1.5$, $\omega_1 = 2$, $v_2 = 1$, $\omega_2 = 4$)

5.3.1.2 Rest of Barrier

Again suppose $\theta_2 = \pi$, but with $x_1 > 0^+$ and $x_2 > 0$, i.e., P and E are initially heading towards each other with P slightly to the right but in front of E. This situation is explained in more detail in [27] but it is obvious that E will turn a hard left and P will turn hard right and since P's initial distance is not as great, P's time, τ_1 (or τ_1'), with a straight control, i.e., $d = 0$, is reduced. Again there is some x_2 distance, not as great as before, for an initial condition which will result in a near miss under optimal play. This is a point on the barrier neighboring the crossover point.

.1 Barrier Types

Barrier trajectories can follow L1, L2, R1, and R2 patterns near crossovers, though for points far from the crossover and thus closer to the capture cylinder, trajectories will

consist of only one segment, though the two crossover types indicate how the rest of the barrier is formed. That is, by varying the parameters τ_1 (or τ_1') up to the crossover switching time when termination corresponds to a UL, and by varying other values for θ_0, barrier points can be collected.

The barrier in the plane of $\theta = \theta_2$ is not in general a feasible trajectory, but comprises the initial conditions for barrier trajectories. Since the BUP is just the reachable set at termination, the left and right barrier must meet the capture cylinder tangentially at the BUP.

In Figure 5.5 and 5.6 are the relative coordinate and real coordinate trajectories of a barrier trajectory for a system where E is twice the speed of P but has half the maximum angular velocity of P. The case considered is one in which P is initially facing towards the right of E, e.g., $\theta_2 = 2.62 rads$. This trajectory type is only one segment and can be thought of as type R1 where $\tau_1' = 0$ and the terminal condition is not at the UL termination.

.2 Case of Identical Vehicles

The basic shape of Merz's barrier is helical and bulges in the middle due to the larger range of collisions when the vehicles are facing each other ($\theta_2 = \pi$) than when they are moving in the same direction ($\theta_2 = 0$ or $\theta_2 = 2\pi$). As θ_2 is varied from 0 to 2π, the crossover point rotates along the reachable set and since they are sharp intersections of the left and right barriers, a sharp ridge rotates along the reachable set. These points form an evader's dispersal line (EDL) and defines the intersection of the left and right barriers.

Symmetry allows construction of Merz's barrier to be concerned with only $\theta_2 \in [0,-\pi]$ and the rest $\theta_2 \in [-\pi,-2\pi]$ is the reverse mirror image through $\theta = 0$, i.e., for $(\theta_2 + \varepsilon) \in [0,-\pi]$ for $\varepsilon > 0$, the barrier is the same shape as $(\theta_2 - \varepsilon) \in [-\pi,-2\pi]$ just rotated $-\varepsilon$ about the cylindrical axis. The EDL and UL are also symmetric . However, for variable v and ω, the DL's and UL's are on different sides of $\theta = 0$, so this case must be treated for all $\theta \in [0,2\pi]$.

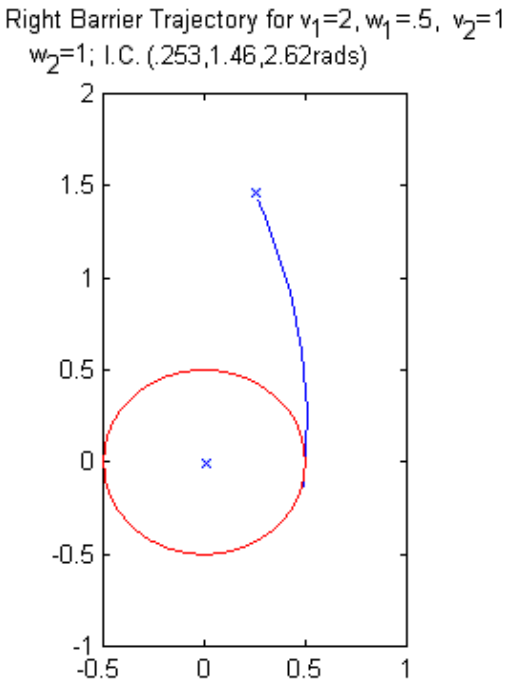

Figure 5.7: Barrier trajectory in game of kind; one segment; case of non-identical vehicles

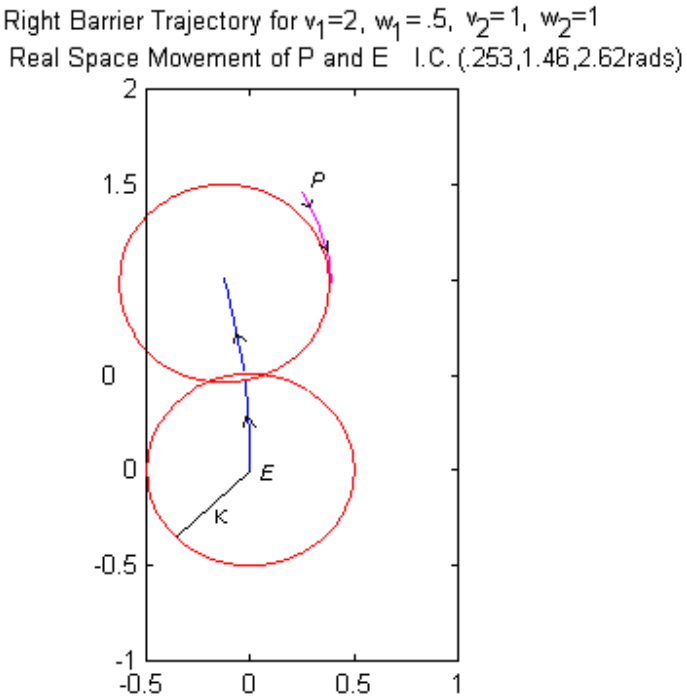

Figure 5.8: Real space trajectory of Figure 5.7; case of non-identical vehicles

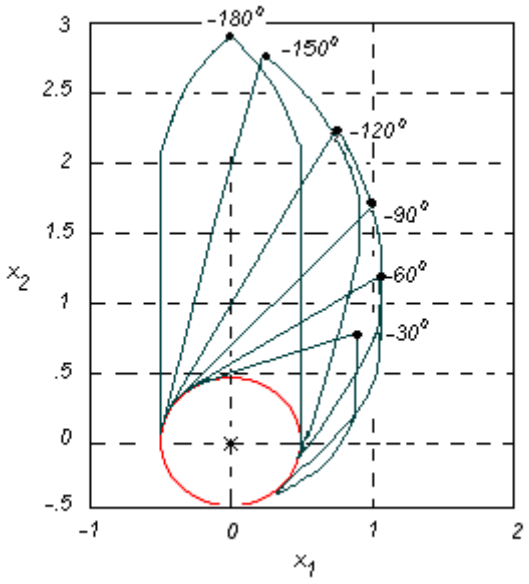

Figure 5.9: Left and right barriers for $\theta_0 \in [0,-\pi]$; case of identical vehicles ($v_1 = \omega_1 = v_2 = \omega_2 = 1$)

5.4 UL and DL Revisit

$u = -1$ throughout the right hand barrier implying no instantaneous strategy is needed for the decision P makes leaving right barrier DL. Similarly, none is needed for the left barrier DL. Also note on a UL, d must take on an intermediate value $d \in (-1,1)$, otherwise the trajectory would pass through the UL and no longer be optimal without switching. To determine the value of d on the UL, we must resort back to the fact that we require $A = 0$, $H^o = 0$, and $\overset{o}{A} = 0$ on this line. From the work and techniques in [32], it can be proved that $d = 0$.

The DL can be determined as the intersection of two sets of retrograde trajectories; those with $\theta_0 < \cos^{-1}\left(\frac{v_2}{v_1}\right)$ and those with $\theta_0 > \cos^{-1}\left(\frac{v_2}{v_1}\right)$. It has been tacitly assumed that these set of trajectories actually intersect, all the way up to the intersection of the left and right barriers. If they did not, a "hole" in what would be a closed reachable set results. Unfortunately, either no sufficiency conditions exist or they just haven't been found yet, so we must check for holes numerically in the construction of the barrier.

We consider an example in setting up the right barrier DL:

Consider point $z_2 = (x_1, x_2, \theta_2)$ on DL. The terminal conditions lie on either side of the DL, so

$$\theta_0 < \cos^{-1}\frac{v_2}{v_1} \qquad \text{and} \qquad \theta_0' > \cos^{-1}\frac{v_2}{v_1}$$

where no prime denotes the left side trajectory (though in this example it is still a right barrier trajectory) and prime denotes the right side trajectory (refer to Figure 5.1). The left side trajectory meets the right side trajectory at z_2. So we may form three equations:

$$\begin{aligned}\kappa \sin\phi_0 \cos\omega_1\tau_2 + \kappa\cos\phi_0 \sin(-\omega_1\tau_2) - R_1(1-\cos\omega_1\tau_2) + R_2(\cos(\theta_0 - \omega_1\tau_2) - \cos\theta_2) \\ = \kappa\sin\phi_0' \cos\omega_1\tau_2' + \kappa\cos\phi_0' \sin(-\omega_1\tau_2') - R_1(1-\cos\omega_1\tau_2') - R_2(\cos(\theta_0' - \omega_1\tau_2') - \cos\theta_2)\end{aligned} \tag{5.12a}$$

$$\begin{aligned}\kappa\cos\phi_0 \cos\omega_1\tau_2 - \kappa\sin\phi_0 \sin(-\omega_1\tau_2) + R_1(-\sin(-\omega_1\tau_2)) - R_2(\sin(\theta_0 - \omega_1\tau_2) - \sin\theta_2) \\ = \kappa\cos\phi_0' \cos\omega_1\tau_2' - \kappa\sin\phi_0' \sin(-\omega_1\tau_2') + R_1(-\sin(-\omega_1\tau_2')) + R_2(\sin(\theta_0' - \omega_1\tau_2') - \sin\theta_2)\end{aligned} \tag{5.12b}$$

$$\theta_0 - (\omega_1 + \omega_2)\tau_2 = \theta_0' - (\omega_1 - \omega_2)\tau_2' \tag{5.12c}$$

where

$$\sin\phi_0 = \frac{v_1 - v_2\cos\theta_0}{W},\ \cos\phi_0 = \frac{v_2\sin\theta_0}{W}$$

and

$$\sin\phi_0' = \frac{v_1 - v_2\cos\theta_0'}{W'},\ \cos\phi_0' = \frac{v_2\sin\theta_0'}{W'}$$

τ_2 and τ_2' are solved for and checked to be sure they are less than $\min\{\tau_A, \tau_3\}$, where τ_A and τ_3 are the times at which A and V_3, respectively, are annulled. Their retrograde solutions can be determined as

$$A = -R_1 u[\cos\phi_0 - \cos(\phi_0 + \omega_1 u\tau)] \tag{5.13a}$$

$$V_3 = R_2 d[\cos(\phi_0 - \theta_0) - \cos(\phi_0 - \theta_0 + \omega_2 d\tau)] \tag{5.13b}$$

Chapter 6

Cost Manipulation for Vehicular Collision

This chapter discusses a variety of approaches to modeling actual vehicular concerns in and around collision avoidance. A couple ways will be through manipulation of the cost function and modifications or additions to the dynamics.

We will not be dealing with any time-varying costs whether they are running or terminal. So, we can trim (3.7) to:

$$J(x,t,u(\cdot),d(\cdot)) = l(x(0)) + \int_t^0 L(x(s),u(s),d(s))ds \tag{6.1}$$

where we have assumed again for convenience $t_f = 0$, and s is a positive running time parameter. We will examine other choices of the index $L(x,u,d)$ to see if changes in the optimal maneuvers might better represent different scenarios. To focus our attention, throughout the remainder of this paper, we will restrict $v_1 > v_2$ since this is the more interesting case.

6.1 Keeping Bounds on a Straight Path

6.1.1 The Straight Path Scenario

For demonstration, suppose a vehicle is traveling straight down a single lane road. Then the left and right edges of the road are essentially bounds in the real space of E. We could also suppose E is traveling in a lane with an adjacent lane for oncoming vehicles. Still bounds can be similarly introduced for E. Other situations might include E traveling amidst a certain number of lanes or traveling in a space between other vehicles.

Thus we add a constraint in E's real state space (x_{1E}, x_{2E}). We will also assume E is behaving optimally, i.e. (3.22a). The goal is to track E's real trajectory with respect to these bounds, and locate the point at which E's control is considered no longer optimal, i.e., E must switch controls to prevent running off the road. We will consider this example of a straight path and demonstrate how it integrates real state bounds into collision avoidance without increasing the dimension of the game. Moreover, it will pave

the way to an analysis of combining path following objectives with collision avoidance objectives.

6.1.2 Defining Bounds in Real Space

Let x_L denote the perpendicular distance from the left edge or left bound in the x_{1E} direction to the vehicle E. Assume the width of the lane is w_R. The figure shows the left and right bounds remain constant for any given x_{2E}, simulating a straight path. We note in this case x_L will be perpendicular to the road's direction. Denote θ_E as the clockwise angle from the positive x_{2E}-axis. We restrict $\theta_E \in \left[-\frac{\pi}{2}, \frac{\pi}{2}\right]$ since we do not desire reverse motion. We could also suppose the initial conditions for E to be $x_L(t_2) = x_L{}^i = \alpha w_R$ and $\theta_E(t_2) = \theta_E{}^i$, where $\alpha \in [0,1]$ and we again use the notation t_2 as a forward initial time. See Figure 6.1.

6.1.3 Example Illustrates Controls Knowledge as Advantage

Assume E is initial heading vertical and is in the middle of the road. So since E moves about a circle of radius $\frac{R_1}{u} = \frac{v_1}{u\omega_1}$, and we can write real space equations for E:

$$x_L(t) = \frac{w_R}{2} + \frac{R_1}{u}(1 - \cos\omega_1 u(t - t_2)) \qquad t \in [t_2, 0] \qquad (6.2a)$$

$$\theta_E(t) = \omega_1 u(t - t_2) \qquad t \in [t_2, 0] \qquad (6.2b)$$

This is just an example to show the advantages of having control a priori. That is, E can easily track itself and predict its future position with respect to some global reference. As a result, a vehicle may be able to predict times-to-switch and when or if to apply brakes.

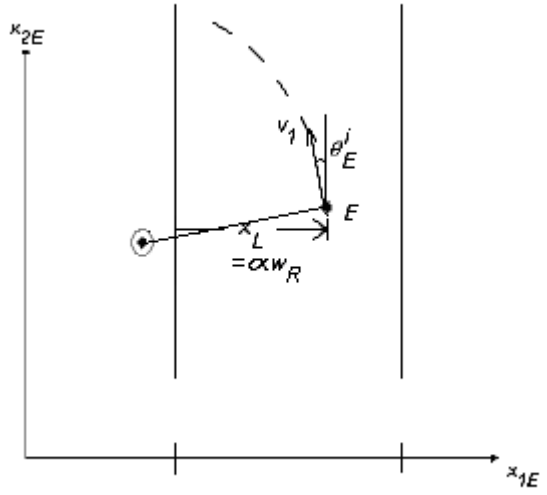

Figure 6.1: Real space tracking of vehicle; e.g. x_L distance to left edge

6.2 Reducing Steering

[36] introduces an entire new cost J_2 over the controls which render the safe set invariant. However, the second cost loses its effectiveness when the initial condition lies inside the unsafe set, i.e., the barrier. However, this thesis will take a different approach and keep one cost over the entire input space. If avoidance is the only objective, then this would be okay, but as we have seen there are other factors and even if a collision seems unavoidable, the game of kind is a worst-case analysis and we would like to prevent the vehicle from making drastic maneuvers.

In this section, we limit the degree of steering through the cost formulation. Since u is attempting to maximize the Hamiltonian, we would like the running cost to be a nonnegative function which reaches a maximum when $u = 0$, i.e., E is heading straight. One could select $L(t,x,u,d) = 1 - u^2$. We reformulate the cost as

$$J = G_0 l(x(0)) + G_1 \int_t^0 1 - u^2 ds \tag{6.6}$$

where we have assigned weights to the terminal and running costs. These are to be adjusted in order to weight avoidance with keeping the vehicle straight. Since E always selects $u = -1$ or $u = 1$ in the game of kind, the effect of the terminal cost and the effect

of the running cost are traded off as the weights are varied. Forming the optimal Hamiltonian,

$$H^o(x,V_x)$$
$$= \max_{u\in[-1,1]} \min_{d\in[-1,1]} \left\{G_1(1-u^2) + p_1(-\omega_1 u x_2 + v_2 \sin\theta) + p_2(-v_1 + \omega_1 u x_1 + v_2\cos\theta) + p_3(\omega_2 d - \omega_1 u)\right\}$$

$$= \max_{u\in[-1,1]} \min_{d\in[-1,1]} \left\{G_1(1-u^2) + A\omega_1 u + v_2(p_1\sin\theta + p_2\cos\theta)) - v_1 p_2 + p_3\omega_2 d\right\}$$

u selects a value such that $G_1 - G_1 u^2 + A\omega_1 u$ is maximized. This maximum occurs at

$$u(x,p) = \frac{A\omega_1}{2G_1} \tag{6.7}$$

Of course, this control is only valid if $\frac{A\omega_1}{2G_1}$ falls in the range $[-1,1]$. If $\frac{A\omega_1}{2G_1}$ moves outside the range $[-1,1]$ in the space of (x,p), the control is clipped at the appropriate extreme. Whereas this overall control scheme is still not differentiable in t, it is now continuous everywhere except at dispersal lines and surfaces where the adjoints become discontinuous.

The first gain G_0 factors into the problem at the boundary point when $t=0$. From Hamilton's necessary conditions, $p_0 = G_0 \frac{\partial l}{\partial x}(x(0)) = (G_0\sin\phi_0, G_0\cos\phi_0, 0)$. This is just a scaled version of that obtained in the game of kind. As long as $G_0 > 0$, there is no change in the terminal controls, but since the control in general is a function of p, the terminal co-state conditions p_0 affect the locations of the barrier and singular surfaces. It is apparent that the reachable set will be smaller due to the added steering cost than that obtained from just a terminal cost.

We could also try $L(t,x,u,d) = 1+\cos\pi u$. The optimal Hamiltonian implies that u is selected such that $G_1 + G_1\cos\pi u + A\omega_1 u$ is maximized. This maximum occurs at $u(x,p) = \frac{1}{\pi}\sin^{-1}\frac{A\omega_1}{\pi G_1}$, and this control is only valid if $|A\omega_1| \le \pi G_1$ (compare to $|A\omega_1| \le 2G_1$ for the previous case).

To test the effect of the addition of the running cost $L(x,u,d) = 1-u^2$, the cost of the system whose barrier trajectory was depicted in Figure 5.5 was replaced but the system was started at the same initial condition. This new trajectory as well as the old is plotted in Figure 6.3. It is seen that for the terminal cost E and P nearly miss each other, while

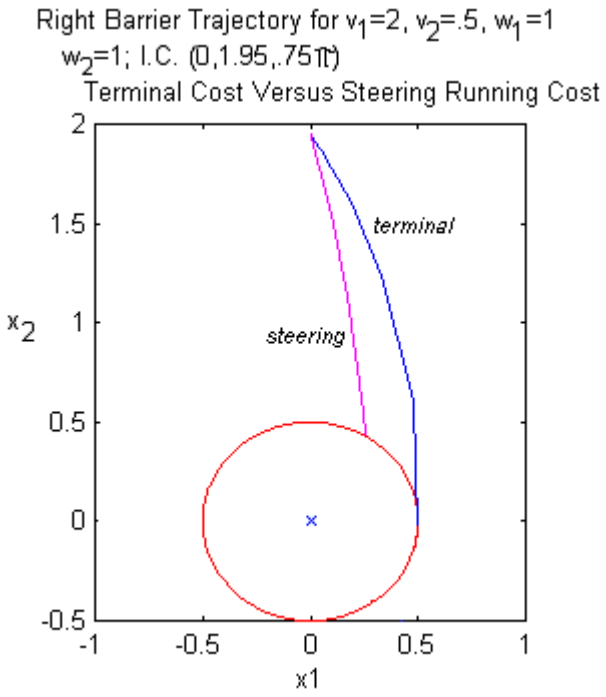

Figure 6.2: Comparison of terminal cost and steering cost for E on a straight path

for the running cost E and P collide. This is a result of the tradeoff which E gives up in order to turn less. We will note this technique is similar to the one introduced in Chapter 4 as a hybrid technique. In the next chapter, we will discuss the advantages and disadvantages of these two techniques.

6.3 The Lateral Model Addition

6.3.1 Augmented State Equations

In order to handle curved road edges, we can take advantage of the lateral control model of a vehicle as introduced in Section 3.1. However, we adjust the relative model to fit a rolling disc to reduce dimension, and redefine the angles θ and θ_t to be subtended clockwise from the global vertical axis. This revises equation (3.3) to

$$\begin{bmatrix} \dot{s} \\ \dot{d}_1 \\ \dot{\theta}_p \end{bmatrix} = \begin{bmatrix} \dfrac{v_1 \cos\theta_p}{1 - d_1 c} \\ v_1 \tan\theta_p \\ -\dfrac{v_1 c \cos\theta_p}{1 - d_1 c} \end{bmatrix} + \begin{bmatrix} 0 \\ 0 \\ \omega_1 \end{bmatrix} u \tag{6.8}$$

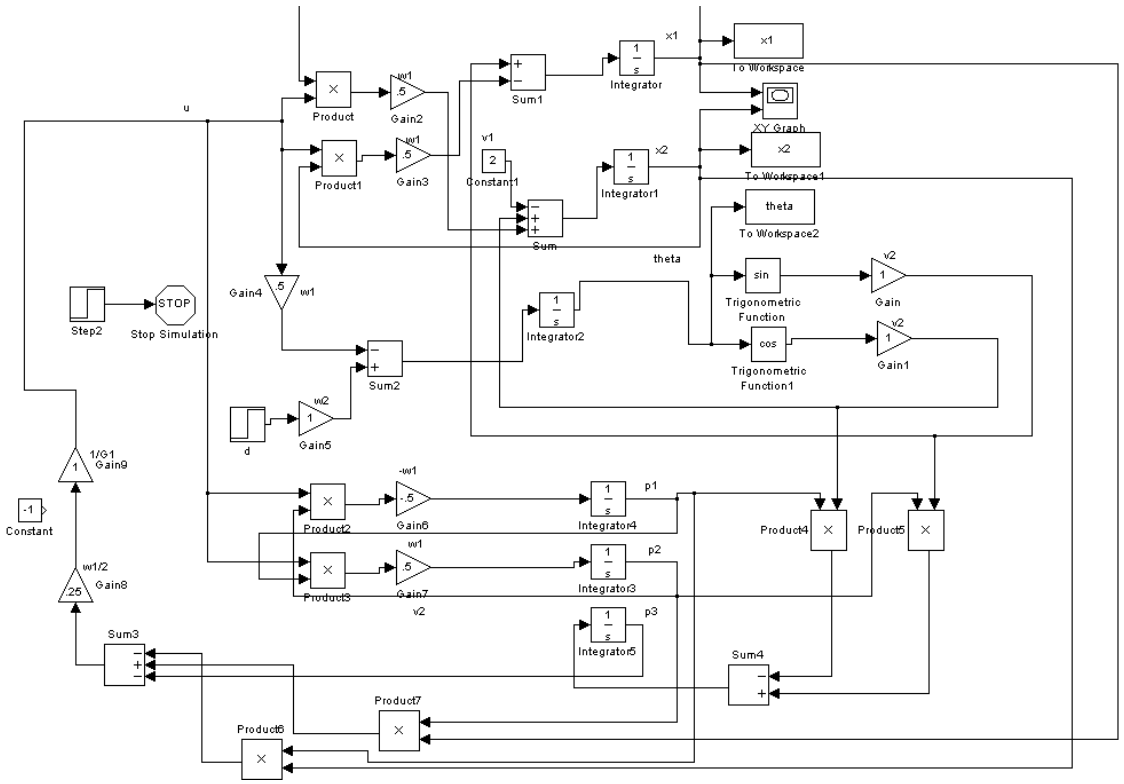

Figure 6.3: Simulink feedback model for steering cost formulation

where again $\theta_p = \theta - \theta_t$ and $c(s) = \dfrac{d\theta_t}{ds}$ is the curvature of a path as a function of the arc length, s. For example, a straight path has curvature $c(s) = 0$ and a curved section of a circle has curvature $c(s) = \pm\dfrac{1}{r}$, where r is the radius. Together c and s represent a parameterization in global coordinates (x_{1E}, x_{2E}) the path to be followed by the vehicle. We still extend the perpendicular of the path's tangent line to the middle of the rear axle and label this distance d_1. Refer to Figure 5.4.

In fact, lateral control, such as in [9] utilize this model to drive d_1 to zero in an effort to have a nonholonomic vehicle follow a certain path and have stability and convergence properties through feedback.

Unfortunately, our system dynamics have increased three dimensions; the combined system being

$$\dot{x}_1 = -\omega_1 u x_2 + v_2 \sin\theta \qquad (6.9a)$$

$$\dot{x}_2 = -v_1 + \omega_1 u x_1 + v_2 \cos\theta \tag{6.9b}$$

$$\dot{\theta} = \omega_2 d - \omega_1 u \tag{6.9c}$$

$$\dot{s} = \frac{\cos\theta_p}{1 - d_1 c} v_1 \tag{6.9d}$$

$$\dot{d}_1 = \tan\theta_p v_1 \tag{6.9e}$$

$$\dot{\theta}_p = \omega_1 u - \frac{c\cos\theta_p}{1 - d_1 c} v_1 \tag{6.9f}$$

If initial conditions for s, d_1, and θ_p are known and the nominal path can be parameterized through some known $c(s)$, then d_1 can be mapped as function of time.

6.3.2 Game of Kind in Six Dimensions

Consider (6.9) with a terminal cost formulation, i.e.,

$$J = l(x(0))$$

where $l(x) = \sqrt{x_1^{\,2} + x_2^{\,2}} - \kappa$ as before. We derive the optimal controls from the new set of state equations through the Hamiltonian, which becomes an augmentation of the three-dimensional state problem:

$$H^o = \max_{d\in[-1,1]} \min_{u\in[-1,1]} \left\{ A\omega_1 u + v_2(p_1 \sin\theta + p_2 \cos\theta) - p_2 v_1 + p_3 \omega_2 d + p_4 \dot{s} + p_5 \dot{d}_1 + p_6 \dot{\theta}_p \right\}$$

which implies

$$u^* = \operatorname{sgn}(A + V_6) \tag{6.10b}$$

$$d^* = -\operatorname{sgn} V_3 \tag{6.10b}$$

Terminal co-state conditions can similarly be determined on the UP and BUP of the capture cylinder as in the original game of kind but with the additions $p_{40} = 0$, $p_{50} = 0$, and $p_{60} = 0$. The process is the same as in the original formulation of the game, i.e., find the terminal optimal controls and run the system back in time until a discontinuity in the adjoints is reached. Moreover, the analytic solutions for (x_1, x_2, θ) are still applicable since the first three states are decoupled from the last three states.

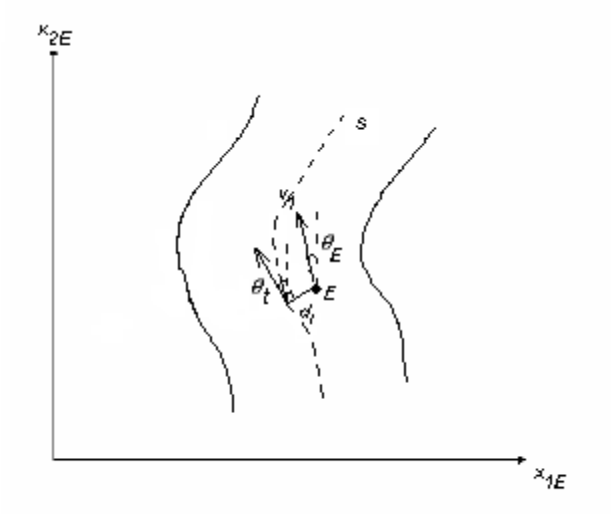

Figure 6.4: Evader's position in path following variables

6.3.3 Cost Formulation

Note in the lateral addition in (6.10) the input appears only in the dynamics of θ_p. This implies, for this setup, that incorporating $\dot{d}_1$ or $\dot{s}$ into the running cost has no direct effect on the optimal controls. However, minimizing $\dot{\theta}_p{}^2$ would in effect not only minimize changes in the steering angle from the road angle, but also somewhat minimize total steering angle deviation when considered over a short duration. We reformulate the cost as

$$J = G_0 l(x(0)) + G_1 \int_t^0 -\dot{\theta}_p{}^2 ds \tag{6.12}$$

The optimal Hamiltonian is the game of kind optimal Hamiltonian with the running cost added within the braces. u selects a value such that

$$-G_1 \omega_1{}^2 u^2 + \left[(A + V_6)\omega_1 + \frac{2G_1 \omega_1 c \cos\theta_p}{1 - d_1 c} v_1 \right] u$$

is maximized. The maximum and its constraints can be found in a similar manner as was done in Section 6.3. Note if $c(s) = 0$, we have the essentially the same cost formulation as the straight path in Section 6.3, with the exception that this system is six-dimensional and the optimal control depends on V_6.

6.3.4 Lateral Addition Considerations

This cost formulation does not account for any state bounds but in effect it may limit the turning enough to avoid moving too far to the left or right. Furthermore, this is handled around any path whose curvature is known or estimated.

Another way to incorporate d_1 into the cost formulation is to free up the constancy of v_1 and allow v_1 to be another input. Now a control appears explicitly in the dynamics of d_1 and thus affects the Hamiltonian. Of course this adds even more complexity and so will not be pursued.

We see that on a straight path, and perhaps even on a curve with a constant curvature, the lateral addition can be thrown out and a quadratic term of the input can be substituted. This is highly desirable since the dimension of the system may remain at three and the reachable set can be constructed similar to Chapter 5.

6.4 Chapter Conclusions

We placed gains on the terminal and running costs for fine tuning according to one's system, and this might have to be done through trial and error. Of course, the effect of either the terminal or running cost can be neglected by allowing its gain to be zero.

We see two ways to consider real bounds and other secondary objectives without increasing the dimension of the problem. First, extrapolating the motion of vehicle, calculations can be done online. Such examples were given in Section 6.3 and 6.4 for a straight path and circular path, respectively. After a certain calculated time period, the control may switch in order to avoid state bounds. Such calculations could be modeled into the system creating an overall hybrid system, where switching controls may correspond to switching hybrid states.

Second, running costs may be added. We could formulate a cost such that steering reduction was coupled with collision avoidance, thus allowing the system to remain at dimension three. We saw an example of this for a vehicle on a straight path. The formulation may also be extended to circular paths without added dimensions. We would like to analyze the system setup and solutions for these running costs, and use the straight path scenario as an example. Whereas the lateral addition dominates in its path following capabilities, the added dimensions increases the complexity more than desired.

Chapter 7

Solution Approach and Implementation

This chapter considers the pros and cons of adjusting the game theoretic approach, as the ones done in Chapter 6, what it means to the problem, and what it implies to further research of applying this approach to a real collision avoidance system. This chapter will also discuss the control strategies, what they mean to the problem, and the other issues relevant to implementation. We will conclude with the data which a real collision avoidance system using this approach may sense.

7.1 Problem Description

So far, we have two main descriptions of the game-theoretic problem and may use either to describe an optimal solution x^* and the associated control strategies u^* and d^*. There is the HJI PDE,

$$\text{(HJI)} \begin{cases} V_t + H^o(x, V_x) = 0 \\ H^o(x, V_x) = \max_{u \in [-1,1]} \min_{d \in [-1,1]} H(x, p) \\ V(x,0) = l(x(0)) \end{cases} \tag{7.1}$$

and Hamilton's set of necessary conditions, i.e.,

$$\text{(HAM)} \begin{cases} \dot{x}^* = f(x^*, u^*, d^*) \\ \dot{V}_x = -\dfrac{\partial H}{\partial x}(x^*, u^*, d^*) \\ \dfrac{\partial H}{\partial u} = 0, \dfrac{\partial H}{\partial d} = 0 \\ x(0) = x_0, p(0) = p_0 \end{cases} \tag{7.2}$$

7.2 Game of Kind Numerical Considerations

The unsafe set, that is, $S_1 \setminus R^n$, maybe thought of as a reachable set, from wherein after a certain amount of time despite the input of E there exists a disturbance which forces the trajectory to reach the target set T. Again, let $t_f = 0$ and $t < 0$ be the initial time of the trajectory. We would like to know for some initial condition if it reaches the target set within the given amount of time, $\tau = -t$. Define

$$G(\tau) = \{x \in R^n \mid \exists d(\cdot) \in D, \forall u(\cdot) \in U, \exists s \in [t,0], \zeta(s;x,t,d,u) \in \text{int}\, T\} \tag{7.7}$$

where $\zeta(s;x,t,d,u)$ is a solution trajectory to the system (3.13).

7.2.1 Method of Computing Unsafe Set

In order to ensure that once a trajectory penetrates the unsafe region, it does not penetrate back into the safe region, (3.29) can be modified [22] to

$$-V_t = \min\left\{0, H^o(x,V_x)\right\} \tag{7.8}$$

This keeps $V_t \geq 0$, so if at some point, $V > 0$, there is no way after some time, $V < 0$, at the same point. Combining this idea and analytic solutions into level set techniques, [22] is able to construct this reachable set for a terminal cost formulation.

The [22] time dependent method has advantages over its convergent competitors in its ability to determine at any point in the state space its "distance", i.e., $|V(x,t)|$, to the nearest point on the boundary of the reachable set, as well as determine if it is inside or outside the boundary. This is an advantage from a control perspective. Its disadvantage is its disability to handle state constraints without incessant reinitialization.

7.2.2 Generalized Solutions and Viscosity Solutions

Analytic solutions cannot be used when the value function is not differentiable, i.e., at shocks. We must introduce viscosity solutions in order to fully describe $G(\tau)$ [22].

To completely solve the HJI PDE requires defining some form of generalized solutions, or solutions which are assumed to be locally Lipschitz on some domain Ω in R^n. Unfortunately, these generalized solutions are not unique in general and some may converge uniformly to a form that is not a solution.

Viscosity solutions fix this uniqueness problem and provide stability properties that otherwise might not be present. Note viscosity solutions are different than vanishing viscosity solutions, which involve approximating the PDE with a quasilinear elliptic equation of 2nd order, i.e.,

$$-\varepsilon\Delta V^{\varepsilon} + H^{o}(x, V^{\varepsilon}, V_{x}^{\varepsilon}) = 0 \tag{7.9}$$

where V^{ε} is the desired solution and ΔV^{ε} is the Laplacian of the solution. The Laplacian is the 2nd order term which defines the "viscosity" of the PDE which is a term well known in the literature of fluid dynamics. As ε is driven to zero, this term will be seen to "vanish".

A viscosity solution, V, is considered "weak" in that it is only assumed to be continuous and V_x may not exist or is discontinuous. The viscosity solution of an HJI can be proven to be the solution to a two-player zero sum differential game [37]. Also, if V is a viscosity solution and locally Lipschitz in Ω, then V is differentiable in Ω and becomes a classical solution. Further properties are described in [38].

Among the set of bounded, uniformly continuous functions, a viscosity solution $V(x,t)$ satisfies $V_t + H^{o}(x, V_x) = 0$, provided that for each infinitely differentiable test function $\psi(x,t)$:

if $V(x_0,t_0) - \psi(x_0,t_0)$ is a local maximum, then $\psi_t(x,t) + H^{o}(x, \psi_x(x,t)) \le 0$
if $V(x_0,t_0) - \psi(x_0,t_0)$ is a local minimum, then $\psi_t(x,t) + H^{o}(x, \psi_x(x,t)) \ge 0$

7.2.3 Level Set Methods

Level set methods were originally designed to compute approximations to the viscosity solution for time dependent HJ PDEs, but can be adapted to the approximation of reachable sets.

Suppose $V : R^n \times [t,0] \to R$ is a viscosity solution of an HJI PDE with a terminal cost, i.e., V is a solution to

$$\begin{aligned} &V_t + \min\{0, H^{o}(x, V_x)\} = 0, && \text{for } t \in [t,0], x \in R^n \\ &V(x,0) = l(x), && \text{for } x \in R^n \end{aligned} \tag{7.10}$$

where $l(x)$ is the terminal cost function and $H(x, V_x) = \max_{u\in[-1,1]} \min_{d\in[-1,1]} V_x f(x,u,d)$ as before.

Then if the zero sublevel set of $l(x)$ describes the target set, then the zero sublevel set of V describes the backwards reachable set $G(\tau)$ as:

$$G(\tau) = \{x \in R^n \mid V(x,t) \le 0\} \quad [22] \tag{7.11}$$

This theorem allows numerical schemes from level sets to compute accurate approximations of V and consequently $G(\tau)$.

Interest lies only in the zero level set of V, which at termination, is the capture cylinder, as seen in $V = l(x(0)) = \sqrt{x_1^{\,2} + x_2^{\,2}} - \kappa$. At previous times the zero level set describes the boundary of the reachable set, or $G(\tau)$, after τ time units have elapsed. Optimal trajectories inside or outside the boundary are on either side of the zero level set; thus, the inside trajectories have $V < 0$ and the outside $V > 0$. With Merz's parameters, $\kappa = 1$, and V defined as the terminal function above, it takes $\tau = 2.5$ time units for the reachable set to approximately reach a steady state set [28].

Using analytic solutions from the terminal condition formulation provides, a large collection of points on the boundary may be found. The PDE solver must generate $V = 0$ for these points. For a point z_i off the boundary, $|V(z_i)|$ is a measure of the error. The error in a level set method is dependent upon the number of grid points and whether interpolation is used in between points or not. [22] demonstrates the convergence properties of its level set method and ODE solver as the number of grid points is increased to 60000 analytic surface points. It is noted that the maximum error is at worst one grid cell and that the average is smaller than 1/10 of a grid cell [22].

7.2.4 Other Game of Kind Considerations

The dimension of the differential game may give problems to the formation and analysis of the barrier if it happens to exceed three. E.g., making velocity a state increases the dimension to four. The dimension problem arise out of the fact that for certain values of v_1, v_2, ω_1, and ω_2, the EDL which encloses the two barriers may leak over the range $\theta \in [0, 2\pi]$. Furthermore, "holes" may be present in the left or right barrier if the retrograde solutions normally colliding to form the DL do not collide [31]. These two situations may give the opportunity for the evader to steer its way out of the "collision set". Thus, the non-existence of leaks and holes must be verified numerically.

7.3 Running Cost Numerical Considerations

7.3.1 Motivation

Numerical techniques are almost inevitable. Even when analytic trajectories can used to locate crossover points, barrier points, universal lines, dispersal lines, universal surfaces, or dispersal surfaces, nonlinear sets of equations must be solved for times-to-go, τ_2 and τ_2', through numerical root finding techniques. However, it is noted that these algorithms are generally faster than a numerical PDE solver [22]. On and around kinks especially require numerical approaches. We will discuss level set methods as a way to approximate the reachable set.

Due to singular lines and singular surfaces in a terminal cost problem, it becomes difficult to apply convergent approximations to the co-state variable p since it is discontinuous across them. The UL's and US are avoided when a running cost is introduced since the optimal input u^* is continuous and not a switch function. However, d^* still contains a switch function, and as a result, the DL's and DS still remain.

7.3.2 Reduced Set of ODE's

Many numerical techniques which may be helpful to this differential game setup are based on Hamilton's set (7.2). The variation of extremals, e.g., assumes a feedback form for the controls, i.e., $u^* = u(x, p)$ and $d^* = d(x, p)$, can be analytically determined, and by inserting these in the set of state and co-state equations, a set of reduced order differential equations can be written, i.e.,

$$\dot{x}^* = f(x^*, u^*(x, p), d^*(x, p)) \qquad x(0) = x_0 \qquad (7.12a)$$

$$\dot{V}_x = -\frac{\partial H}{\partial x}(x^*, V_x, u^*(x, p), d^*(x, p)) \qquad V_x(0) = p_0 \qquad (7.12b)$$

where again $t_f = 0$. By moving around extremals with different initial and final conditions, iteratively a solution may be obtained.

We note that (7.12a) and (7.12b) are now coupled together, i.e., in order to project a trajectory back we must solve both (7.12a) and (7.12b), unlike the situation with a terminal cost. Moreover, through the Hamiltonian we can acquire optimal controls. And as long as we can terminate the game, optimal controls give us a set of ODE's in which the boundary conditions are no longer split. Then we may use an ordinary ODE solver.

7.3.3 Solution through Method of Characteristics

We could also use the method of characteristics to help solve optimal trajectories from a running cost. In Chapter 3, we found the set of ODE's from this method to be

$$\dot{x}^* = f(x^*, u^*, d^*) \tag{7.13a}$$
$$\dot{t} = 1 \tag{7.13b}$$
$$\dot{V} = -L(x^*, u^*, d^*) \tag{7.13c}$$

As an example, we consider the addition of the cost of steering from Section 6.2, i.e., we let $J = G_0 l(x(0)) + G_1 \int_t^0 1 - u^2 ds$. We found $u^* = \frac{A\omega_1}{2G_1}$ and $d^* = -\operatorname{sgn} V_3$. Equation (7.13c) produces

$$\dot{V} = \frac{A^2 {\omega_1}^2}{4G_1} - G_1 \tag{7.14}$$

The vehicle is assumed to be heading on a straight path. The set of ODE's through the method of characteristics is the same as Hamilton's set with the addition of the dynamics of V. Note $\dot{V} \le 0$ for $|u| \le 1$, so over time V is never increasing, or V remains constant or is decreasing to its value at the capture cylinder. Unless E is heading straight, $\dot{V} < 0$. This will be the case since u^* is continuous and not a switch function and thus there are no singular surfaces for E. There still remains, however, DL's and the DS since d^* hasn't changed.

7.4 Control Design

7.4.1 Terminal Cost Control Design

From a control perspective, E only needs to know the initial condition. If the initial condition lies on the left barrier, $u = 1$, or if on the right barrier, $u = -1$. And for the cases on the EDL, E could play a mixed or bias strategy. If it lies inside the barrier as determined through some technique, then similarly E plays a strategy depending on the US. Nonetheless, despite u^*'s dependence upon the state and co-state of the system, with just the initial condition, E knows its strategy until termination, assuming optimal play.

One possible way to determine where the initial condition resides with respect to the barrier is to look at the initial orientation θ_2 and form the left and right barriers in this

constant plane of θ. The bad part about this is that computing these barriers for a given θ_2 may require many computations since barrier trajectory types must be distinguished, then barrier points collected, and finally the DL or DS constructed; and all done online. Note for a given θ_2, the barrier always tapers as it moves away from the origin. Thus, if one could find a barrier trajectory such that the line between the origin and barrier point included the initial condition, then this would indicate the region. One idea might be to rely upon an iterative procedure; i.e., compute an initial barrier point and iteratively move towards the initial condition by either going up or down the barrier side.

From a control perspective, E doesn't necessarily have to play optimally until the trajectory reaches the barrier. However, within a certain distance, E may want to begin control as if P was on the barrier, perhaps to account for uncertainties. One way, which might complement the nearby barrier point calculation, is after it is determined the initial condition lies outside the barrier, whichever barrier side is closer its control is applied, i.e., $u = 1$ for the left barrier and $u = -1$ for the right barrier.

7.4.2 Running Cost Control Design

As discussed in Section 7.4.2, u^* and d^* are continuous functions of the state and co-state. Again, we can consider situations inside or outside the barrier, not just on the barrier. Furthermore, we can produce retrograde trajectories in order to locate barrier points and manage an appropriate control. The main difference is analytic techniques fail in this case and rather than applying a control just based off initial condition, we must first solve the set of ODE's (7.12). This is certainly a disadvantage to the running cost addition.

7.4.3 Downfall of Lateral Addition

The lateral addition not only adds three dimensions but much is obscured intuitively. In game of kind or degree, a terminal condition is selected, i.e. near miss or collision, and ran the system back optimally to see the set of initial conditions which would lead to this terminal condition. However, for a six-dimensional system, a terminal condition must include values for d_1, s, and θ_p which indicates a terminal lateral state which the vehicle is in. Individual cases do not easily provide enlightening information on a collision scenario and so one would have to form a set of terminal conditions, as d_1, s, and θ_p varies. Thus computation has increased dramatically which could have been one terminal condition and one or two retrograde trajectories in the original game of kind or degree.

Projecting trajectories back in time from their terminal conditions for outside the barrier cases becomes complex in the same manner, i.e., terminal conditions are selected and they could come from any given r, not just $r = \kappa$ as in original game of kind and degree.

7.5 FLASH Vehicle Setup

The FLASH lab is devoted to research and small-scale simulation of an automated vehicle. Current vehicles have four main levels: sensors, high-level processor, low-level processor, and actuators (motor and servo). With the low-level processor taking the burden off the high-level by driving the motor and servo, and with the variety of sensors, the high-level processor is capable of many different control schemes and algorithms.

7.5.1 Sensors

Sensors are integral to the success and performance of any collision avoidance system. Whereas we will not discuss the sensor types, various methods of operations, or sensor performance, we would like to mention what data would be necessary for this differential game setup. First, sensors at least must be capable of identifying and locating the (x_1, x_2) initial position and orientation θ_2 of a threat P. Sensors also must indicate P's real linear velocity v_2, and P's maximum angular velocity ω_2, all of which could be approximated e.g., by measuring P's position shortly after initial recognition. Certain assumptions and criteria could also be constructed for these parameters; e.g., ω_2 could be overapproximated more so than v_2 since the former is considered a maximum value. Of course, the vehicle has lesser trouble determining v_1 and ω_1.

Once the initial state and the two rolling disc parameters for each player are set, a differential game could be run. If E is lane bounded, a few more parameters might be needed. On a straight path, the vehicle might keep track of x_L at all times during the avoidance maneuver as well as its real heading direction θ_E. However, if E's initial offset and orientation are known, x_L and θ_E can be calculated rather than sensed. If however on a curved portion of a road, it may be necessary for E to continually sense this data if no a priori knowledge of the future road's shape is known.

7.5.2 Current Sensors

Table 7.1 lists all of the working sensors available on the FLASH vehicle. The vehicle is capable of path following through either infrared detection of a white line, magnetic detection of magnets placed directly underneath the infrastructure, or through camera

detection (which has not yet been implemented). The car utilizes ultrasonic sensors to detect the presence of another vehicle in its application of adaptive cruise control.

Component	Model	Manufacturer
Reflective object sensor	QRD1114	Fairchild Semiconductor
Hall effect sensor	HAL506UA-E	Micronas
CMOS image sensor	OV7610	OmniVision
Ultrasonic scanner kit	3-705	Mondo-tronics

Table 7.1: FLASH vehicle sensors

7.5.3 Sensors for Collision Avoidance

Infrared sensors could be a cheap route to simulate an actual vehicle's method of distance measurement, which may not be infrared but maybe laser or radar. As long as the sensors onboard the FLASH vehicle remains fast and accurate with respect to its environment, one could simulate a slower system by adjusting the sampling rate.

Reflective sensors could be used if an object could be encased with reflective material. The FLASH vehicle currently utilizes these kinds of infrared sensors, as shown in Table 7.1. These sensors may operate at distances of 50-200mm, which will probably be too short to consider avoidance maneuvers on the current track with the current vehicle's velocity.

Ultrasonic sensors and infrared range-finders provide detection of objects at further distances. While the range-finders can detect from 10cm to 80cm, the ultrasonic sensors can detect from 150mm to 2.67m. On the other hand, range-finders produce less error in detection and consume less power. Moreover, ultrasonic sensors tend to be bigger in size and more expensive. Nonetheless, it is assumed ultrasonic would provide the best simulation component for the FLASH vehicle.

Chapter 8

Conclusions and Future Work

8.1 Conclusions

This chapter describes the conclusions generated and contributed to collision avoidance systems and the possible routes for future work.

1. The application of a game-theoretic approach to collision avoidance may be extended to include non-identical vehicles (or possibly planes, ships, etc.) in which $v_1 \neq v_2$ and $\omega_1 \neq \omega_2$. This is due to the similar analysis and setup for a representation of the safe and unsafe sets in state space, and determining the optimal controls, trajectory types, singular lines and surfaces, and methods for solving the value function.

2. This thesis is tailored to vehicular collision avoidance on automated highways. As such, there are certain parameters which may be introduced (and sensed) in order to aid in collision avoidance maneuvering with respect to the road and available space provided by the road.

3. Whereas 2nd objective cost functions have been previously introduced [36], this thesis took a new approach by integrating other parameters into a single cost function. The results indicated some advantages such as continuity of control, absence of universal lines and surfaces, while disadvantages included loss of analytic techniques and necessity to solve co-state equations. .

4. There are several approaches to reducing the steering during avoidance. This may be accomplished in a hybrid manner with multiple terminal cost formulations, permitting analytic solutions, or through one cost with a running weight, permitting continuous controls.

5. In general adding running costs or increasing dimension without specifying boundary conditions creates too broad a problem and may obscure any meaning behind a safe and unsafe set. It is believed to preserve these characteristics while further reducing assumptions would require bounding the problem in some manner, e.g., using hybrid techniques.

8.2 Future Work

There is much room for improvement, modification, and new techniques left to be employed in the area of vehicular collision avoidance. Even with three dimensions a good deal of work is needed to divide the state space into a safe and unsafe set.

It would be worthwhile to test the validity of the setup(s) in this paper on some test bed such as the one devoted to FLASH research. This may provide measures in verifying the success of a game-theoretic approach in optimizing safety.

Whereas vehicles would not likely implement the discussed controllers directly, testing may approve or decline further analysis with this method. If successful, and it is believed this approach provides optimal solutions, further improvement may be accomplished with the introduction of time-varying velocities, or in essence, modeling braking..

References

[1] *Traffic Safety Facts 1998*. National Highway Traffic Safety Administration, Report #DOT HS 808 956.

[2] *Traffic Safety Facts 2002*. National Highway Traffic Safety Administration, Report #DOT HS 809 640.

[3] M. Bellis. *The History of the Automobile*. http://inventors.about.com/library/weekly/aacarssteama.htm. 2002.

[4] A. De Luca, G. Oriolo, C. Samson. *Robot Motion Planning and Control* Chapter 4. http://www.laas.fr/ jpl/book.html. Dec. 1999.

[5] E. Moret. *Dynamic Modeling and Control of a Car-Like Robot*. Thesis. Virginia Polytechnic Institute and State University, 2002.

[6] R. D. Henry. *Automatic Ultrasonic Headway Control for a Scaled Robotic Car*. Thesis. Virginia Polytechnic Institute and State University, 2001.

[7] R. Tribe, K. Prynne and I. Westwood. *Intelligent Driver Support*. Proceedings of the 2nd World Congress on Intelligent Transportation Systems, Vol III, pp. 1187-1192, November 9-11, Yokohama Japan.

[8] A. Gorjectani, C. Shankwitz, M. Donath. *Impedance Control for Truck Collision Avoidance*. Proceeding of American Control Conference, June 2000, Chicago, IL.

[9] P. Mellodge. *Feedback Control for a Path Following Robotic Car*. Thesis. Virginia Polytechnic Institute and State University, 2002.

[10] M. Egerstedt, X. Hu. *A Hybrid Control Approach to Action Coordination for Mobile Robots.* Brief Paper Division of Engineering and Applied Science, Harvard University, Cambridge, MA, 19 June 2001.

[11] T. Belker and D. Schulz. *Local Action Planning for Mobile Robot Collision Avoidance.* IEEE/RSJ Intl. Conference on Intelligent Robots and Systems. EPFL, Lausanne, Switzerland. October 2002.

[12] J. Borenstein and Y. Koren. The vector field histogram – fast obstacle avoidance for mobile robots. IEEE Journal of Robotics and Automation, 7(3): pp. 278-288, 1991.

[13] G. Wanielik, N. Appenrodt, H. Neef. *Polarimetric Millimeter Wave Imaging Radar And Traffic Scene Intrepretation*

[14] C. Chen and R. Quinn. *A Crash Avoidance System Based upon the Cockroach Escape Response Circuit*. Proceedings of the IEEE International Conference on Robotics and Automation. Albuquerque, NM, April 1997.

[15] O. Azouaoui, M. Ouaaz, A. Chohra. *Fuzzy ArtMap Neural Network (FAMNN). Based Collision Avoidance Approach for Autonomous Robotic Systems (ARS).* Second Workshop on Robot Motion and Control, October 18-20, 2001.

[16] J. Jansson and F. Gustafsson. *Decision Making for Collision Avoidance Systems.* Society of Automotive Engineers, Inc., 2002.

[17] D. Swaroop, String Stability of Interconnected Systems: *An Application to Platooning in Automated Highway Systems.* Ph.D. dissertation, Dept. Mech. Eng. Univ. California, Berkeley, 1994.

[18] P. Varaiya, *Smart Cars on Smart Roads: Problems of Control.* IEEE Trans. Automat. Contr.,vol. 38, no. 2, pp. 195-207, 1993.

[19] C. J. Tomlin, J. Lygeros, S. S. Sastry *A Game Theoretic Approach to Controller Design for Hybrid Systems*. IEEE.

[20] J. Hu, J. Lygeros, M. Prandini *Aircraft Conflict Prediction and Resolution Using Brownian Motion.* Proceedings of the 38th Conference on Decision & Control Phoenix, Arizona, December 1999.

[21] G. J. Pappas, C. Tomlin, S. Sastry *Conflict Resolution for Multi-Agent Hybrid Systems*. Proceedings of the 35th Conference on Decision and Control Kobe, Japan, December 1996.

[22] I.M. Mitchell. Application *of Level Set Methods to Control and Reachability Problems in Continuous and Hybrid Systems*. PhD Dissertation. August 2002.

[23] P.L. Lions. *Generalized Solutions of Hamilton-Jacobi Equations.* Pitman Advanced Publishing Program University of Paris, Dauphine, 1982.

[24] R. Vinter. *Optimal Control.* Edwards Brothers, Inc., Ann Arbor, MI, 2000.

[25] D. S. Naidu. *Optimal Control Systems.* CRC Press, Pocatello, ID, 2003.

[26] McOwen. *Partial Differential Equations.* 2nd Edition, 2000.

[27] A.W. Merz. *Game of Two Identical Cars.* Journal of Optimization and Application, Vol. 9, No. 5, 1972.

[28] I.M. Mitchell. *Games of Two Identical Vehicles.* September 4, 2001.

[29] D. D. Kirk. *Optimal Control Theory.* Prentice-Hall, NJ, 1970.

[30] E.C. Zachmanoglou and D.W. Thoe. *Introduction to Partial Differential Equations with Applications.* Williams and Wilkins Co., MD, 1976.

[31] T. Basar and G.J. Olsder. *Dynamic Noncooperative Game Theory.* Academic Press, New York, 1982.

[32] R.P. Isaacs. *Differential Games.* John Wiley and Sons, Inc., NY, 1965.

[33] I. Mitchell and C. Tomlin. *Level Set Methods for Computation in Hybrid Systems.* In B. Krogh and N. Lynch, editors, Hybrid Systems: Computation and Control, number 1790 in Lecture Notes in Computer Science, pages 310-323. Springer Verlag, 2000.

[34] C. Tomlin, J. Lygeros, and S. Sastry. *A Game Theoretic Approach to Controller Design for Hybrid Systems.* Proceedings of the IEEE, 88(7):949-970, July 2000.

[35] D. Peng, B. Merriman, and S. Osher. *A PDE Based Fast Local Level Set Method.* Journal of Computational Physics, 165:410-438, 1999.

[36] C. Tomlin, G.J. Pappas, and S. Sastry. *Noncooperative Conflict Resolution.* Proceedings of the 36th Conference on Decision and Control San Diego, CA, 1997.

[37] L. C. Evans and P. E. Souganidis. *Differential Games and Representation Formulas for Solutions of Hamilton-Jacobi-Isaacs Equations*. Indiana University Mathematics Journal, 33(5):773-797, 1984.

[38] M.G. Crandall and P.L. Lions. *Viscosity Solutions of Hamilton-Jacobi Equations.* Trans. Amer. Math. Soc.

[39] M. Falcone. *Numerical Solution of Dynamic Programming Equations. In Optimal Control and Viscosity Solutions of Hamilton-Jacobi-Bellman Equations*. Birkhaauser, 1997.

[40] C.L. Navasca and A.J. Krener. *Solution of Hamilton Jacobi Bellman Equations.* Proceedings of the 39th IEEE Conference on Decision and Control Sydney, Australia, December 2000.

Vita

I, Christopher "Corey" Howells was born in Huntington in the wild, wonderful state of West Virginia. I obtained a BSEE at Virginia Tech, cooped with General Electric Fanuc at Charlottesville, VA, and continued on into the masters program at Virginia Tech. One summer I was privileged to work with the Corp. of Engineers as hydrologic technician gathering water quality data and calibrating field and home equipment. I intend to continue into the doctoral program in EE at Virginia Tech, but to what field I will be research is still unknown, but exciting to think about.